UILU-ENG 89-3603

Report No. 149

STRUCTURE, CHEMISTRY, AND ELECTROCHEMICAL BEHAVIOR OF MIXED METAL (RUTHENIUM, TITANIUM) OXIDES

by

Joseph E. Suarez and J. M. Rigsbee
Department of Materials Science and Engineering

A Report of the

MATERIALS ENGINEERING—MECHANICAL BEHAVIOR

College of Engineering, University of Illinois at Urbana-Champaign

May 1989

ABSTRACT

This study focuses on the structure-chemistry-property relationships of ruthenium-titanium-oxide films deposited onto niobium substrates by reactive ion plating, a plasma assisted physical vapor deposition technique. A range of microanalytical techniques including SEM, TEM, electron microprobe, Auger microprobe, x-ray diffraction, and electron diffraction was used to characterize film microstructure, morphology, and chemistry. Film electrochemical activity was studied via anodic polarization testing. A relationship was shown to exist between oxygen flow rate and source evaporation rates, and resultant film microstructure, chemistry, and crystal phases. Solid solutions of ruthenium in TiO_2 (rutile) and TiO (cubic) formed at average oxygen flow rates below 95 sccm. Films with a dual phase mixture of RuO_2 and TiO_2 (rutile) were produced when average oxygen flow rates were equal to or exceeded 95 sccm. The presence of TiO_2 (anatase), with TiO_2 (rutile) and RuO_2, was shown to be related to a lowering of the ruthenium evaporation rate and a corresponding decrease in overall ruthenium (and RuO_2) content. Films comprised of 80-90 at.% titanium (20-10 at.% ruthenium) in the form of a dual phase mixture of RuO_2 and TiO_2 (rutile) exhibited the greatest degree of electrochemical activity of those films fabricated and tested for the study, i.e. they possessed the ability to maintain a stable flow of current with little to no rise in applied potential for extended periods of time. Electrochemical activity was diminished in those ruthenium-titanium-oxide films containing either TiO_2 (anatase) with TiO_2 (rutile) and RuO_2, or ruthenium in solid solution with TiO_2 (rutile) or TiO (cubic). There is evidence suggesting the possibility that a TiO_2 (rutile)-to-TiO_2 (anatase) phase transformation is induced by anodic polarization in films containing both TiO_2 (anatase) and TiO_2 (rutile). It is also suggested that an amount exceeding 5 at.% ruthenium is required to stabilize the rutile form of TiO_2 in films comprised of RuO_2 and TiO_2. The study shows that a combination of ruthenium depletion and

substrate oxidation are mechanisms by which the oxide films on niobium lose their electrochemical activity under anodic polarization.

ACKNOWLEDGEMENT

The author thanks Dr. J. Michael Rigsbee for the opportunity to participate in graduate study at the University of Illinois. Dr. Rigsbee's support, guidance, and friendship have been very important throughout the author's tenure at the University. The U. S. Army Construction Engineering Research Laboratory is acknowledged for the use of their ion plating facility. The University of Illinois' Center for Microanalysis of Materials is acknowledged for access to their facilities. The assistance of Ms. Nancy Finnegan and Mr. John Woodhouse are much appreciated. Thanks are also extended to Mr. Cameron Begg for use of the Department of Geology's electron microprobe. The author extends special thanks and appreciation to Mr. Mihir M. Shah whose teaching, advice, prodding, and friendship were most welcome through the course of this investigation. Thanks are also extended to Mr. John H. Givens for his help, advice, and friendship. Financial support for this research program was provided, in part, through U. S. Army Corps of Engineers contract DACA88-88-M-1039.

TABLE OF CONTENTS

I. INTRODUCTION

The focus of the research program centers on the structure-property-processing relationships associated with mixed metal (ruthenium, titanium) oxide films deposited onto niobium substrates using the reactive physical vapor deposition technique of ion plating. Ruthenium-titanium-oxide (RTO) films deposited onto metallic substrates known as valve metals, i.e. metals with the inherent ability to form self-passivating, electrically insulating surface oxide films, find application as anodes in the electrolytic production of chlorine, electroplating, and impressed current cathodic protection. A high degree of electrochemical activity under anodic polarization conditions is desirable in these films. Electrochemical activity refers, in this instance, to the RTO film's ability to maintain a stable flow of current under anodic polarization with little to no increase in applied potential for extended periods of time. The main objective of the research effort is twofold: (1) determine the interrelationships between microstructure, microchemistry, and film electrochemical activity, and (2) ascertain the relationship between electrochemical activity, structure, and chemistry of the oxide films and those ion plating process parameters responsible for the specific structures and chemistry/phases obtained. Specific questions addressed by the study include:

A. How do variations in ion plating process parameters affect film microstructure and chemistry/phases;

B. What is the correlation between electrochemical activity, microstructure, and chemistry/phases;

C. What is the sequence of events responsible for decreases in electrochemical activity and film failure.

Reactive ion plating, a modification to conventional ion plating where the glow discharge contains a reactive gas such as oxygen in

addition to the inert gaseous component, was chosen as the deposition technique for the fabrication of RTO films because of its ability to produce adherent, dense films with high temperature microstructures and phases at relatively low deposition temperatures. Structure-property relationships were determined through the use of a number of analytical tools and techniques including scanning and transmission electron microscopy, x-ray and electron diffraction, electron microprobe, Auger electron spectroscopy, and anodic polarization testing. Data derived from these studies pertaining to variations in morphology, microstructure, and chemistry/phases were correlated to the ion plating process parameters which effected them. Data pertaining to film electrochemical activity, and subsequent changes in morphology, microstructure, and chemistry/phases resulting from polarization testing, and consequently affecting film activity, was documented. Based upon the aforementioned data, a processing window was defined from which RTO films exhibiting properties desirable for impressed current anodes, i.e. devices through which current is made to flow by the application of an external power supply, could be produced and reproduced.

II. REVIEW OF LITERATURE

A. CATHODIC PROTECTION

The earliest reported development of cathodic protection occurred in 1824 following the demonstration by Sir Humphrey Davy of preferential accelerated corrosion of one of two electrically coupled dissimilar metals immersed in water. Noting the effect of the (galvanic) corrosion cell he had created, Davy postulated that copper sheathed wooden naval ship hulls would be protected against corrosion through their electrical coupling to iron or zinc plates [1, 2]. From electrochemical theory it is now known (though not in Davy's day) that dissolution of a metal is due to the electrical potential difference created either by the electrical coupling of two dissimilar metals or by the variations in potential which occur across a metal's surface when immersed in an electrolyte. This potential difference results in the flow of current from the anodic electrode or anodic region on the metal's surface to the cathodic electrode or cathodic region resulting in the dissolution (corrosion) of the anodic portion of the corrosion cell. The basic corrosion phenomenon at the anode is expressed in the following electrochemical reaction:

$$M \Rightarrow M^{n+} + ne$$

where

M = metal
M^{n+} = metal ion
e = electron
n = constant

The equivalent electrical circuit diagram of the basic corrosion cell is given in Figure 1 where R_a is the resistance associated with the anodic region and the anolyte, R_c is the resistance of the cathode and catholyte, R_m is the resistance of the metal, and E_a and E_c are the anodic and cathodic potentials respectively.

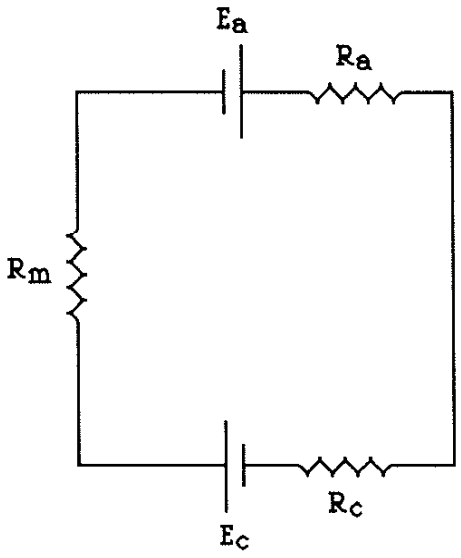

Figure 1: Schematic diagram of a basic corrosion cell [1]

In theory the anodic (corrosion) reaction can be halted by reducing the anodic current, i_a, to zero or to a negative value. It is possible to achieve this state by reducing substantially the potential difference between the anodic and cathodic regions of the corrosion cell. In practice this is accomplished by supplying a flow of current to the normally anodic region of the cell via either a suitable galvanic couple (to a sacrificial anode) or by an external DC power supply electrically connected to an auxiliary anode [2]. This action, in theory, mitigates corrosion by allowing the open circuit potential of the cathodic region to be polarized to the open circuit potential of the anodic region thus forcing the anodic region cathodic with respect to either the sacrificial or auxiliary anode. Ruthenium-titanium-oxide films on niobium substrates function as auxiliary anodes, therefore a discussion of corrosion mitigation through the use of sacrificial anodes is not included in this text.

Schematically the direct current source can be represented by the addition of an external circuit to the basic corrosion cell depicted in Figure 2.

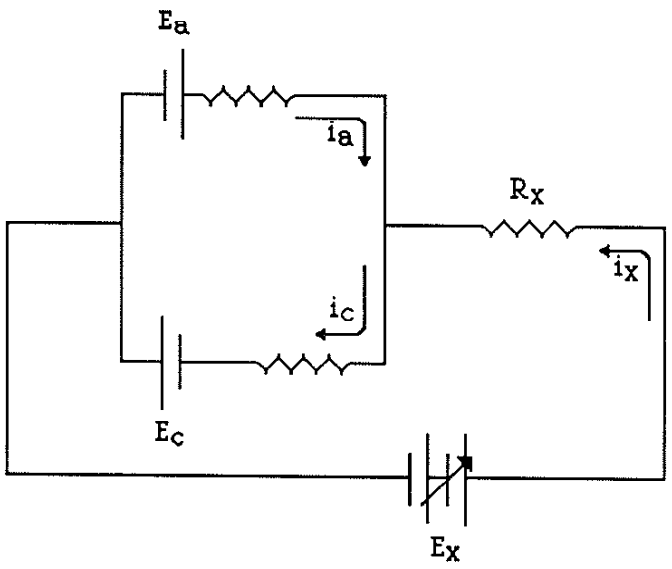

Figure 2: Schematic diagram of the basic corrosion cell with the addition of an external circuit [1]

Applying Kirchoff's law to the circuit given in Figure 2 yields the following expression [1]:

$$i_a + i_x - i_c = 0$$

where i_a, i_x, and i_c correspond to the anodic, external circuit, and cathodic currents, respectively.

It follows that

$$E_a - E_c = i_a R_a + R_c i_c.$$

Substituting for i_c and setting $i_a = 0$ yields the following result:

$$E_a - E_c = R_c i_x.$$

While the above equations do not accurately represent true polarization conditions in a corrosion cell they are illustrative of the basic point, to wit, that an impressed external current, i_x, will reduce the potential difference between the anodic and cathodic regions of the corrosion cell resulting in corrosion mitigation. If the external current, i_x, is greater than that required to reduce the anodic current, i_a, to zero the anodic current will be reversed thereby forcing the normally anodic region of the corrosion cell to act as a cathode which also prevents the onset of corrosion. Application of an external current source for the purpose of decreasing anodic current by reducing the potential difference between cathodic and anodic regions of the corrosion cell results in corrosion mitigation and is the basis behind impressed current cathodic protection [1, 2].

Consumption rates of the auxiliary anodes employed in an impressed current cathodic protection system should be low to maintain effective corrosion protection over long periods. Figure 3 illustrates a basic impressed current cathodic protection system.

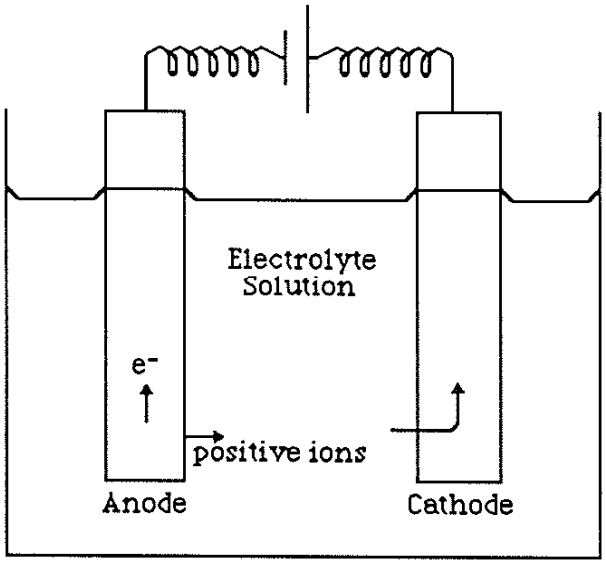

Figure 3. Schematic of a basic laboratory impressed current cathodic protection system [1]

B. MIXED METAL OXIDE ANODES

Combinations of conductive precious (noble) metal oxides and valve metal oxides deposited as a film onto valve metal substrates are currently employed as anodes for the electrolytic production of chlorine, electroplating, and impressed current cathodic protection systems. Henri Beer was the first to use and subsequently patent several precious metal-valve metal-oxide systems for their application as conductive anodic electrodes [3]. Beer's original work in solid solution combinations of precious and valve metal oxides formed the basis for the development of conductive ceramic anodes. The terms "ceramic anode" and "mixed metal oxide anode" (MMO), when referring to anodic films comprised of precious and valve metal oxides, are used interchangeably throughout the cathodic protection and chlor-alkali industries and are thus used in this text in the same manner.

The materials traditionally used commercially as anodic electrodes in the field of impressed current cathodic protection are graphite and high silicon, chrome-bearing cast iron (HSCBCI). Both types of anodes are used in the cathodic protection of metallic structures in salt and fresh water (chlorine and oxygen evolving environments, respectively) as well as in soil. Disadvantages associated with graphite and HSCBCI anodes are: extreme weight (in certain cases exceeding 24 kg); brittleness; difficulty in machining; and, high dissolution rates (≈200 g/A/yr) [4]. Other common anode materials used in impressed current cathodic protection include magnetite, platinum and its alloys, platinized titanium and niobium, and lead.

Mixed metal oxide anodes were introduced into the United States in 1968 [5]. While their compositions vary, most exhibit low dissolution rates (0.005 times less than graphite and HSCBCI anodes), good mechanical properties, acid resistance, high electrochemical activity, corrosion resistance, and longevity [1, 4, 6]. Desirable properties of MMO anodes include:

1. low electrical resistance;
2. a nonporous film with a high electronic transference number to provide an effective barrier to oxygen ions; and
3. an active surface area which will not passivate [7].

1. MMO Anodes of Ruthenium and Titanium

A complete or even adequate phase diagram of the RuO_2 - TiO_2 binary system is not available. Much of the initial work in deriving a diagram was performed by Roginskaya et. al [8, 9] however the end product lacked sufficient detail and is of little use for predicting phase compositions under most conditions. Much of the literature devoted to this binary system contains conflicting information with regard to the specific phases present under given conditions and to the existence and extent of solid solubility between its end members. Consider the following conflicting claims: one paradigm supported by experimental evidence indicates that RTO films containing the rutile phase of TiO_2 can only be nucleated and grown on titanium substrates when using conventional thermal decomposition coating techniques. Conversely, equally strong experimental evidence is found in the literature documenting the presence of RTO films containing TiO_2 (rutile), also deposited via thermal decomposition, onto substrates other than titanium. The observed microstructures and phase compositions for the RuO_2 - TiO_2 system are generally attributed to the crystal structure of the substrate, the processing technique and processing parameters used in film fabrication, and to the specific film precursors. Conflicting results have arisen because, in many instances, such claims were made without completely considering how variations in processing parameters, deposition technique, and the chosen method of deposition affect film growth, structure, and chemistry. Many of these studies are discussed in a subsequent section of the text.

The physical and electrochemical properties exhibited by MMO coatings is to a large extent a function of the methods employed in their fabrication. Traditionally MMO films have been fabricated via the thermal decomposition of organometallic precursors which are

first brushed onto various valve metal substrates and subsequently annealed in air or oxygen atmospheres at temperatures ranging between 300°C - 800°C. Alternative methods used to produce MMO films include chemical vapor deposition and reactive ion plating. A description and study of the chemical vapor deposition technique is beyond the scope of this text, however, an excellent account of the specific methods used by Triggs et. al is given in reference 10.

2. MMO Films by Thermal Decomposition

Several significant studies have been performed pertaining to the microstructural and chemical characteristics of RTO films and the overall dependence of each on processing conditions. Hine et. al. [11] deposited thick films consisting of RuO_2 and TiO_2 onto titanium substrates and glass substrates through the thermal decomposition of $RuCl_3$ and tetra-n-butyl titanate ($Ti(OBu)_4$). Solutions of these coating agents deposited onto titanium plate formed a film consisting of RuO_2 and TiO_2 (rutile). The MMO film was characterized, via x-ray diffraction, as a solid solution with a rutile crystal structure. This is a plausible claim when considering the Hume-Rothery rules for the formation of a solid solution. These same coating solutions deposited onto glass substrates resulted in a film containing TiO_2 (anatase) instead of the rutile form observed on titanium which lead Hine et. al. to conclude that the titanium substrate was necessary for the formation of the rutile oxide phase. O'Leary and Navin [5] claim that the surface layer of TiO_2 (rutile) which forms on oxidized titanium metal serves as a seed to initiate the growth of the TiO_2 (rutile) phase as opposed to the anatase structure. In addition, O'Leary and Navin have found that formation of interfacial layers consisting of titanium suboxides ($Ti_{1-x}Ru_xO_2$, where $0 \leq x \leq 2$) brings about a gradual transition from the titanium metal phase to the oxide phases.

Using solutions of ruthenium hydroxide chloride and titanium chloride as precursors for the generation of RuO_2 - TiO_2 (rutile) films on titanium, Lebedev et. al. [12] postulated that the rutile phase formed as a result of an interaction between a RuO_2 - TiO_2 solid solution and the oxidized titanium substrate. The study concluded that solid solutions of RuO_2 and TiO_2 coexist with a rutile TiO_2 phase

throughout the RuO_2 - TiO_2 system with the exception of a narrow region ($\leq 8\%$ TiO_2) where TiO_2 was said to be soluble in RuO_2. In addition, no evidence of a RuO_2 - TiO_2 solid solution was found for films deposited onto substrates other than titanium.

The results given above conflict with those reported by Gerrard and Steele [13]. Films prepared from $RuCl_3 \cdot xH_2O$ and $TiCl_4$ in isopropanol were deposited onto silica substrates. In both cases TiO_2 (rutile) diffraction peaks were observed. This result prompted the authors to conclude that a titanium substrate was not required to promote and stabilize the rutile crystal structure. The presence of TiO_2 (rutile) was attributed instead to additions of $RuCl_3$ (5-10 mol%) to the $TiCl_4$-isopropanol precursor. Gerrard and Steele believe that $RuCl_3$ has a stabilizing effect on the rutile structure. In addition, this study found no evidence of significant solid solution between RuO_2 and TiO_2 (rutile) for specimens produced at or above 700°C. Instead diffraction peak splitting was observed at these processing temperatures indicating that the films were comprised of separate RuO_2 and TiO_2 (rutile) rich phases. Roginskaya, Bystrov, and Shub [8] showed that a complete transition from the solid solution regime occurs between 900°C and 1050°C as evidenced by the formation of distinct RuO_2 and TiO_2 (rutile) phases.

Single crystals of RuO_2 - TiO_2 fabricated by Triggs et. al., through the use of a chemical vapor deposition technique, were characterized as highly ordered crystals containing RuO_2 and TiO_2 (rutile) rich phases [10]. Evidence of this claim was shown dramatically through back scattered SEM images of the crystals. The ruthenium rich phase appeared as a series of white platelets aligned in only two directions within a titanium rich matrix phase. Because the densities of the two phases differ, Triggs was able to discern each phase in the back scattered images.

From the preceding discussion it is evident that oxide films of ruthenium and titanium, which have various microstructures and phase compositions, can be produced under a variety of processing conditions. Note that conflicting information regarding phase compositions, microstructures, and microchemistry for the RuO_2 - TiO_2 system abounds. Documented "definitive" determinations with

respect to the relationship between the observed properties of ruthenium-titanium MMO films and their structure and chemistry may therefore lack accuracy and be in need of further scrutiny before they acquire widespread acceptance.

3. Ion Plated MMO Films

Little attention to date has been given to the fabrication of MMO films via plasma assisted physical vapor deposition (PVD) techniques. One such PVD technique which has been used to produce MMO films on various substrates is reactive ion plating. With the reactive ion plating technique, Hock, Stephenson, Givens, and Rigsbee deposited RuO_2 - TiO_2 films and niobium-doped titanium oxide films onto niobium, 1018 steel, and glass substrates by electron beam melting pure ruthenium, titanium, and niobium metals into a DC-generated oxygen-argon plasma [6]. Preliminary characterization data pertaining to the niobium-doped titanium oxide films deposited onto all three substrate materials indicated that the film morphology was dense and columnar. The films were characterized as a microcrystalline metal oxide consisting of niobium in solution with both anatase and rutile TiO_2. The RuO_2 - TiO_2 films, which were also deposited onto all three substrate materials, were characterized as a microcrystalline mixed oxide of RuO_2 and TiO_2 (rutile) with a morphology similar to that described for the niobium-doped titanium oxide films. The microcrystalline structure of the films was attributed to the high oxygen partial pressure and/or high oxygen-argon total pressure within the ion plating deposition chamber during film fabrication.

4. Film Electrochemical Activity

By their very nature underground and/or submersible structures are not easily or readily observed in-situ. It is therefore imperative that impressed current cathodic protection anodes maintain their electrochemical activity over a significant period of time. Maintaining electrochemical activity refers to the anode's ability to continually provide a constant flow of current (and thus a constant current density) with little or no rise in applied potential

while subjected to anodic polarization conditions. There are several mechanisms by which MMO anodes loose their electrochemical activity.

One mechanism by which MMO anodes based on RuO_2 - TiO_2 films experience losses in electrochemical activity during anodic polarization is attributed to the formation of a nonconducting oxide film at the MMO coating-valve metal substrate interface. This insulating film has been shown to cause an increase in the resistance at the MMO coating-valve metal substrate interface which is manifested by the potential increase required to sustain a constant flow of current. In addition, differences in the lattice parameters between the deposited MMO film and the valve metal oxide film can effect spalling of the MMO coating thus destroying the anode. Though it is a fundamental characteristic of valve metals to form a potentially deleterious electrically insulating surface oxide film, it is precisely this characteristic which makes the valve metal a superior substrate for MMO anodes. If the MMO coating is mechanically damaged the valve metal substrate, in theory, will form an insulating oxide film on its exposed region. The film serves to halt the flow of corrosion current on the exposed area and therefore keeps the substrate from going into solution. While a portion of the anode passivates, current continues to flow through the active MMO coating allowing the impressed current cathodic protection system to continue functioning.

Formation of the valve metal oxide film at the MMO coating-valve metal substrate interface may occur because of the effect of an induced electrostatic field within the MMO coating during polarization. The field can cause metal or oxygen ions to migrate through the deposited coating toward the valve metal substrate surface thereby providing the ionic species necessary for the formation of an insulating oxide film [14]. Substrate oxidation can also occur in those areas where pores or cracks in the MMO film allow contact of an electrolyte with the substrate surface.

A second important mechanism affecting film activity pertains to the loss of some or all of the constituents comprising the MMO film. Such action can occur during anodic polarization and has a

detrimental effect on anode performance. For RuO_2 - TiO_2 films the effect is evidenced by ruthenium depletion. RuO_2 contributes heavily to the electronic conduction exhibited by these films and thus a lowering of its content reduces the ability of the anode to maintain a constant current flow without increasing the applied potential.

The dissolution behavior of RuO_2 - TiO_2 films under anodic polarization has been studied by Hock, Stephenson, Givens, and Rigsbee [6]. Analyses of the electrolyte by mass spectrometry have shown appreciable quantities of ruthenium in solution [15]. While similar claims are found in the literature no explanation is given for the mechanism by which the preferential dissolution of ruthenium occurs.

In reporting results of x-ray spectroscopic analyses performed on anodically polarized RuO_2 - TiO_2 films deposited onto titanium, Loucka has shown that the film's ruthenium content can decrease to roughly 20% of its original value [16]. The actual RuO_2 and TiO_2 contents are not listed in the documented study, however, the mass ratio of ruthenium to titanium is given as 1:1. Loucka contends from thermodynamic calculations that it is possible for RuO_2 to be oxidized forming RuO_4 (gas) resulting in the dissolution of the major conductive component of the film. A more detailed explanation of this mechanism is given by Elina [17] but is beyond the scope of this text.

It should be recognized that the dissolution of film components and substrate oxidation (which was discussed earlier) are not necessarily independent processes. Both processes may occur simultaneously or sequentially under polarization conditions. Understanding the mechanisms by which MMO films loose their electrochemical activity is an initial step toward effecting changes in their design which can eventually result in impressed current anodes with increased service lives.

5. Titanium and Niobium as Substrate Materials

Titanium and niobium have been recognized as valve metals exhibiting superior physical, electrical, and electrochemical

(corrosion) properties with respect to other valve metals considered as potential substrate materials for impressed current ceramic anodes [7]. Breakdown, i.e. dissolution, of oxidized titanium occurs between 50-60 V (vs. the saturated calumel electrode (SCE)) in electrolytes containing low chloride concentrations with low chloride-to-sulphate ratios. Breakdown of the passivating film on titanium in chloride-rich environments occurs at 10 V (vs. SCE) [18]. Conversely, the passivating oxide film which forms on niobium can withstand applied potentials up to 50 V (vs. SCE) in a salt water electrolyte without going into solution [7]. The breakdown voltage of niobium is said to exceed 120 V [4]. A ceramic anode comprised of a MMO film deposited onto a niobium substrate should, theoretically, possess the ability to withstand greater applied potentials than its titanium counterpart, and thereby supply greater current flow to its surrounding electrolyte and ultimately to the structure for which cathodic protection is being provided. Titanium, however, is utilized much more than niobium as a substrate material for MMO anodes (including anodes consisting of RuO_2 and TiO_2 films) for two reasons. First, the cost of niobium is roughly eighteen times greater than that of titanium. Second, attempts (by commercial vendors) to deposit MMO films onto niobium via thermal decomposition techniques have proven unsuccessful to date.

C ION PLATING

Ion plating is a plasma assisted physical vapor deposition technique which blends the elements of vacuum evaporation and sputtering with the presence of a glow discharge. Mattox introduced the ion plating deposition technique in 1963 [19] and subsequently described it as a film deposition process in which the substrate surface and/or the depositing film is subjected to a flux of high energy particles sufficient to cause changes in the interfacial region or film properties as compared to deposited films fabricated through non-bombarded deposition processes [20]. A complete, detailed account of the ion plating process is given by Ahmed [21].

Ion plating is a high vacuum deposition process performed in a vacuum chamber evacuated to a base pressure of roughly 10^{-6} Torr. Resistance heating, sputtering, or thermionic electron beam evaporation are used to transform solid source materials, from which film atoms are derived, into their vapor states. When a thermionic electron beam evaporation system is used to melt and vaporize source material a dual chamber design, such as the one introduced by Chambers and Charmichael [22], is necessary to create a pressure differential within the vacuum chamber. Pressures approaching 10^{-5} -10^{-6} Torr are common in the lower chamber region housing the electron gun filaments while an alternate pressure of approximately 10^{-2} Torr is present in the upper chamber during deposition. Substrates are fixed to a negatively biased electrode located in the upper chamber and positioned adjacent to the glow discharge.

The glow discharge is generated by either a direct current (DC) or radio frequency (RF) alternating current source electrically connected to the substrate holder. The choice of a DC or RF generated glow discharge is a function of both the conductivity of the substrate material(s) and the desired/required discharge intensity. A primary function of the glow discharge is to ionize the inert and reactive gases within the vacuum chamber thereby causing the negatively biased substrate, and deposited film atoms, to be continually bombarded by energetic ions and neutrals. Energetic particle bombardment results in the desorption or sputtering of surface contaminants from the substrate, i.e. sputter cleaning, increased density of active nucleation sites and substrate defects, increased mobility of adsorbed film atoms, and sputtering and redeposition of the film atoms themselves.

A DC glow discharge is ignited when a potential difference exists between the cathode (the negatively biased electrode which also serves as the substrate holder) and the anode (the grounded vacuum chamber) of an ion plating system containing approximately 3 mTorr of inert and/or reactive gas(es). A pressure approximately equal to 10^{-2} Torr is required to sustain the glow discharge. Subsequent ionization of the inert and/or reactive gas(es) results from electron-atom collisions. The ions undergo charge exchange

collisions with neutral particles within the glow discharge as they are accelerated toward the cathode. The ion-to-neutral particle ratio has been estimated at 0.05%-2.0% [23, 24] which indicates that the glow discharge consists primarily of energetic neutrals. A recent study by Machet et. al. [25] focusing on the ion energy distribution in ion plating processes has shown that, for typical chamber pressures and simple substrate geometries, ions impacting the substrate have average energies of approximately 10%-20% of the applied potential. Average energies of ions and energetic neutrals subjected to a 3 kV bias in a typical ion plating system are reported to be 300 eV and 135 eV, respectively [21].

An RF glow discharge is primarily used for depositing films onto substrate materials which are electrically insulating. The effectiveness of an RF bias lies in the fact that when applied, it serves to reverse the anode/cathode roles every half cycle thus preventing a charge build-up on insulating substrates. The RF generated glow discharge behaves in a similar manner to its DC counterpart [26, 27]. A full explanation of RF glow discharge processes is beyond the scope of this text (a complete account is given by Chapman [26]) but suffice it to say that during RF biasing both electrodes develop a negative bias and both are therefore subjected to particle bombardment. Note, however, that the electrode serving as the substrate holder is much smaller in size than the second electrode, i.e. the vacuum chamber. This asymmetry in electrode dimensions causes the substrate holder to develop a greater bias with respect to the vacuum chamber, subjecting the substrate holder to the high energy particle flux (generated via the glow discharge) and thus to the sputtering process, just as it is under a DC generated bias.

Figure 4 describes pictorially the events occurring during the ion plating process. Mattox [20] has divided the ion plating process into three stages: the initial stage incorporates those processes occurring prior to actual film deposition; the second stage is concerned with interface formation, and the final stage with film growth. Sputtering, the removal of surface atoms via momentum exchange with energetic particles, occurs prior to film deposition. Its

function during the initial stage of ion plating is to remove contaminant atoms from the substrate surface, alter the chemistry of compound substrates by preferentially sputtering one constituent with respect to another, create surface topography, and induce lattice defects or crystalline disorder. Continued particle bombardment during film deposition results in mixing, recoil implantation, and radiation enhanced diffusion, all of which promote the formation of chemically graded interfaces. Particle bombardment further serves to influence the morphology of the growing film as well as effect the formation of high temperature microstructures/phases at low deposition temperatures.

There are many benefits derived from the use of ion plating. Films deposited via ion plating typically display excellent adhesion. High adhesion is a function of (1) the sputter cleaning process which serves to provide a clean and active substrate surface, and (2) the interfacial mixing of film and substrate atoms which occurs during the initial stages of deposition. Depositing films onto substrates having complex and obscured surfaces is also possible by ion plating. The ability to deposit film atoms onto surfaces which are not line-of-sight with respect to the evaporant flux is due to increased gas scattering resulting from the use of a soft vacuum within the upper chamber. Because molecular bonds can be dissociated by the glow discharge it is possible to induce reactions between various species of film atoms and/or between film atoms and reactive gases. For example, when film atoms are introduced into an oxygen and/or nitrogen glow discharge, various oxide, nitride, or oxy-nitride films can form on the substrate surface. In addition, alloys/compounds comprised of elements having zero solid solubility are successfully combined and deposited via ion plating. The fabrication of such materials is possible because ion plating involves atom-by-atom growth and is therefore not subject to the same thermodynamic constraints associated with the formation of bulk materials by conventional solidification techniques.

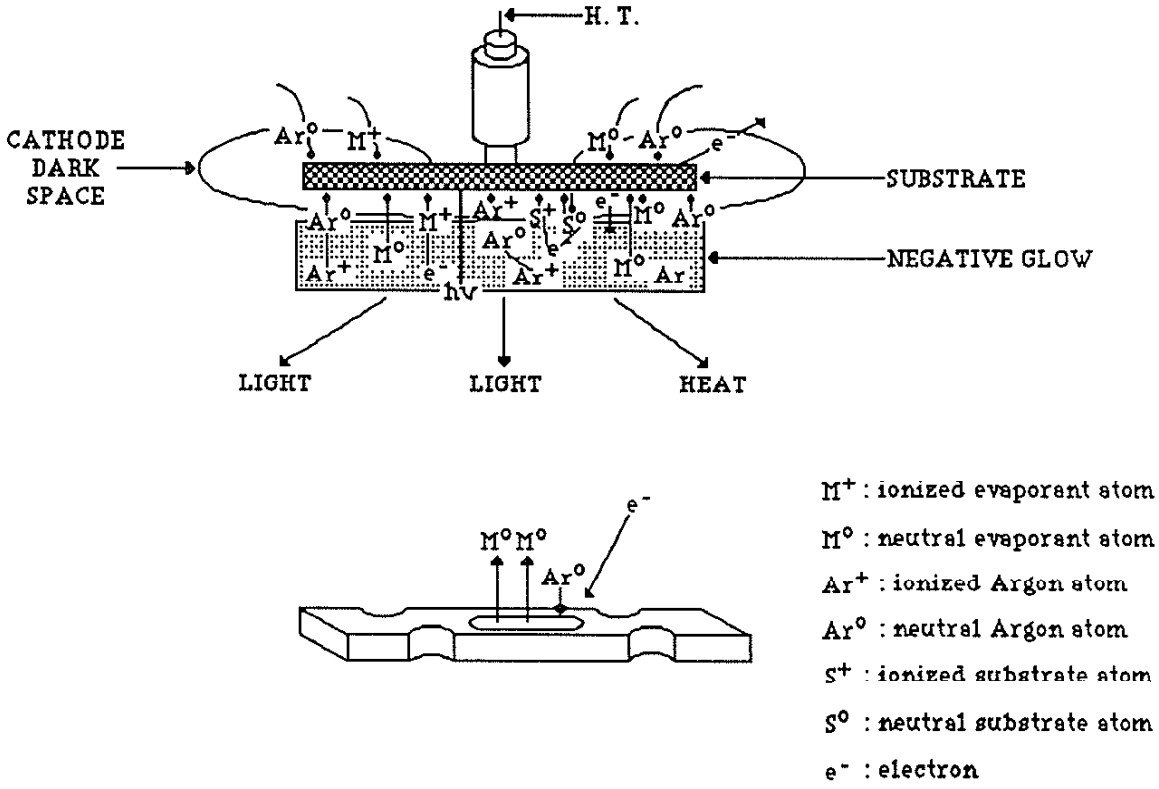

Figure 4. Schematic of the events occurring during the ion plating process [21]

III. EXPERIMENTAL PROCEDURE

A. MATERIALS DESCRIPTION

The solid source material used to grow oxide films of ruthenium and titanium consisted of 99.95% ruthenium powder (120 mesh) and 99.7% titanium rod (1 m lengths, each of which was 6.4 mm in diameter) purchased from Johnson Matthey, Aesar, Inc., Seabrook, NH. The ruthenium powder was formed into 150 g, 35 mm diameter solid compacts via vacuum hot pressing in a Vacuum Hot Press Sintering Furnace Series 3600 manufactured by GCA Corporation, Vacuum Industries Division. The ruthenium powder was consolidated in an inert argon atmosphere and held at $0.6T_{mp}$ with 34.5 MPa uniaxial (hydraulic) pressure for 60 minutes; the same uniaxial pressure was maintained throughout the cooling cycle. Further consolidation of the ruthenium took place in the ion plater as the compacts were electron beam melted and then allowed to solidify. The titanium rod was sectioned into 25 mm lengths using a water cooled silicon carbide abrasive saw. After washing the titanium sections in ultrasonic baths of methanol and acetone each section was placed in the ion plater's water cooled copper crucible for electron beam melting and consolidation.

The substrates used in this study consisted of Corning 7059 borosilicate glass slides (with dimensions of 25.4 mm x 25.4 mm x 1 mm) and unannealed, 99.94 % niobium rod (1 m lengths, 25.4 mm in diameter) purchased from the Cabot Corporation, Boyertown, PA. The niobium rod was machined into 25.4 mm diameter discs, each 5 mm thick, having a tapped hole with an 8-32 thread for mounting. Further preparation of these substrates is discussed in a later sub section.

B. THE ION PLATING SYSTEM

Each of the RTO films used for this study was deposited in the ion plating system located at the U. S. Army Corps of Engineer's Construction Engineering Research Laboratory (USA - CERL), Champaign, Illinois. The ion plater, manufactured by Innotec, Inc. (formerly Torr Vacuum Products, Inc.), utilizes a split chamber design with the upper chamber raised and lowered by a power driven hoist. The upper chamber has the freedom of motion to pivot about its hoist axis allowing access to the system's substrate holder (cathode), gas inlet port, copper crucibles (which serve as the hearths in which the solid source material is placed), and the baffle plate which separates the upper and lower chambers and isolates the electron gun assemblies from the greater pressures maintained in the deposition region of the system. The chambers themselves are cylindrical in shape and each has an inner diameter of 0.66 m. The substrate holder/cathode is a water cooled cylindrical disc which is welded to a pipe that extends through the lid of the upper chamber. The cathode/pipe assembly can be raised or lowered to vary the source-to-substrate distance by loosening a machined teflon block which is designed much like a conflat feedthrough. The teflon block serves to electrically isolate the cathode from the chamber and is responsible for maintaining the vacuum seal at the cathode/pipe-assembly-to-chamber junction. All other vacuum seals excepting the conflat feedthroughs are viton O-rings. Visual inspection of in-situ deposition is made possible by the addition of two 115 mm diameter viewports located on the upper chamber. Several additional ports are available for the mounting of peripheral equipment.

The ion plater's vacuum system is comprised of a 254 mm diffusion pump connected in parallel to a 152 mm diffusion pump, both of which are backed by a single rotary pump. Liquid nitrogen, fed to the traps of each diffusion pump, is used to increase the pumping efficiency of the system.

Solid source material is evaporated in two diametrically opposed water cooled copper crucibles via thermionic electron beam

gun assemblies, each of which is equipped with a magnetic beam deflection system. The electron guns themselves are powered by an Airco Temescal CV-14 Power Supply which is typically operated at ten kilovolts with 0.1 - 0.6 Amperes at each electron gun.

The glow discharge is ignited and intensified with an RF Plasma Products Inc. HFS 1000 G radio frequency (RF) generator which is electrically coupled to the cathode assembly. The RF power supply operates at a frequency of 13.56 MHz and has an incident power capacity of 1.6 kilowatts. The USA - CERL ion plater has the capability of providing a triode enhanced DC generated glow discharge, but this capability was not utilized for the present study. The high purity gases which comprise much of the glow discharge are transported to the deposition chamber via stainless steel conduits. Integrated into the gas transport system are calibrated mass flow controllers capable of varying individual gas flow rates from 0-100 standard cubic centimeters per second (sccm). A titanium gettering furnace is used to further purify high purity argon before it enters the deposition chamber. In addition to argon, nitrogen and oxygen are available as glow discharge constituents and are generally used in the reactive ion plating process. Dry industrial grade nitrogen, admitted to the deposition chamber through a vent valve, is used pressurize the ion plating system to ambient (atmospheric) pressure prior to opening the upper chamber for specimen exchange.

Monitoring consumption rates of reactive gases during reactive ion plating is accomplished through the use of an Inficon Model 1000 residual gas analyzer (RGA). Prior to film deposition consumption curves, which compare the variation in reactive gas ion current and pressure to increasing gas flow rates and electron beam gun current, are generated to indicate the gettering characteristics of the vaporized source material with respect to a particular reactive gas. During the deposition of RTO films the live time data generated by the RGA was used in conjunction with capacitance manometer readings of upper chamber pressure to assess the degree of chemical reactivity between the ruthenium and titanium source materials with the high purity oxygen gas. An RGA used in concert with a

capacitance manometer can also provide the data necessary to calculate the partial pressures of individual gases in the deposition chamber. A schematic diagram of the USA - CERL ion plating system is given in Figure 5.

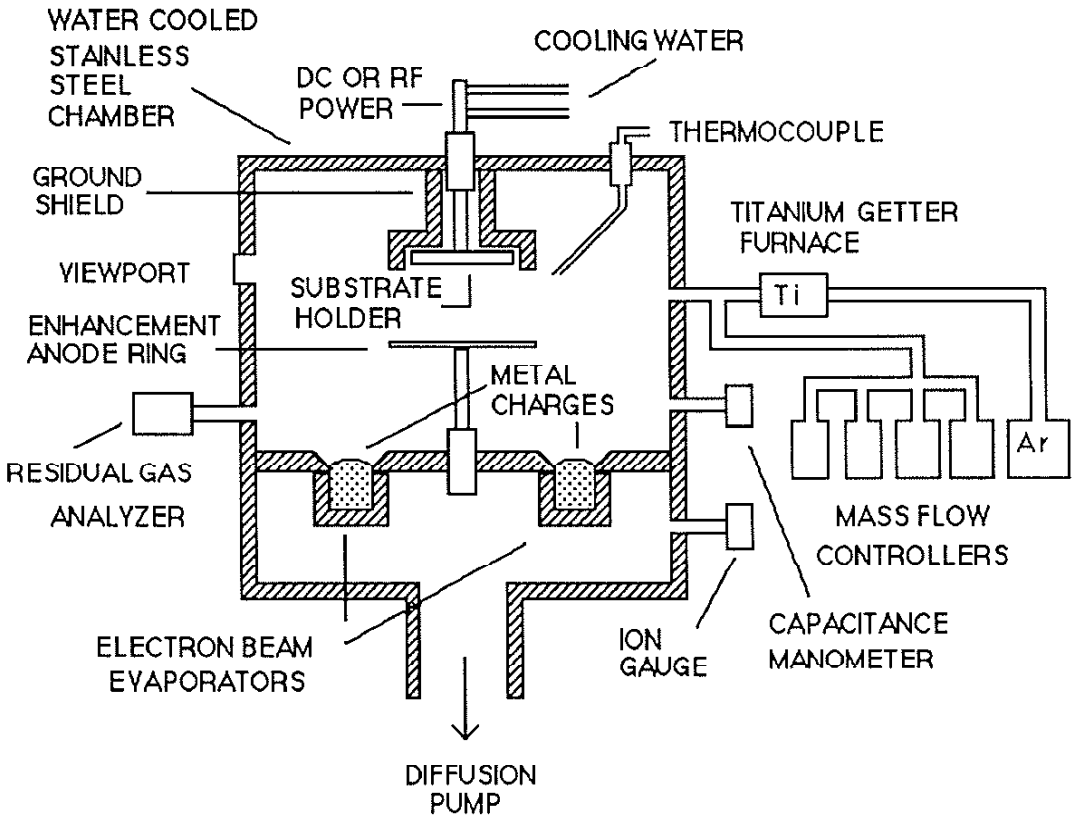

Figure 5. Schematic of the USA - CERL ion plating system.

C. DEPOSITION PROCEDURE

Prior to film deposition the upper chamber of the ion plating system was cleaned and lined with aluminum foil. Since the USA - CERL ion plater is not dedicated to the deposition of one material system, the aluminum foil serves as a disposable liner allowing for quick cleanup between two deposition series and minimizes the extent of contamination from the various material systems under

investigation. Cleaning of the chamber was followed by the loading of source material into the copper crucibles. No substrates were mounted for the initial run. The goal of the initial run was twofold: first it served to melt, further consolidate, and stabilize the source material used in actual deposition runs and second, it provided, via the vaporization of the source material, a coating on the aluminum foil liner of film constituents (in this case ruthenium and titanium) which decreased the probability of contaminating the material system with xenoatoms generated through backsputtering. Consumption curves pertaining to the reactivity of the source materials with the reactive gas(es) were derived and examined upon completion of the initial run to determine potential processing windows, i.e. a plausible range of processing parameters, which result in deposited films with the desired microstructure, chemistry, and observable properties.

Recall from the previous section that consumption curves compare the variation in reactive gas ion current and pressure to increasing gas flow rates and electron beam gun current from which data pertaining to the gettering characteristics of the vaporized source material, with respect to a particular reactive gas, is obtained. Figure 6 is a plot of the oxygen ion current (read from the RGA) as a function of the oxygen flow rate at constant ruthenium and titanium evaporation rates. The oxygen ion current reading is significant in that it represents the amount of unreacted (residual) oxygen remaining in the upper chamber during deposition. The relation between oxygen ion current and unreacted (residual) oxygen is easily seen by noting the direct correlation between the oxygen ion current and the total system pressure (measured by the capacitance manometer) as given in Figure 6. Note also that electron beam gun current values are shown in Figure 6. The ruthenium and titanium evaporation rates are correlated to gun current readings, therefore any changes in the gun current readings represent similar changes in evaporation rates and also in oxygen gettering. A knee in the curves appears at an approximate oxygen flow rate of 70 (sccm). Below this point the ruthenium and titanium are in competition for oxygen while above the point the system is oxygen saturated.

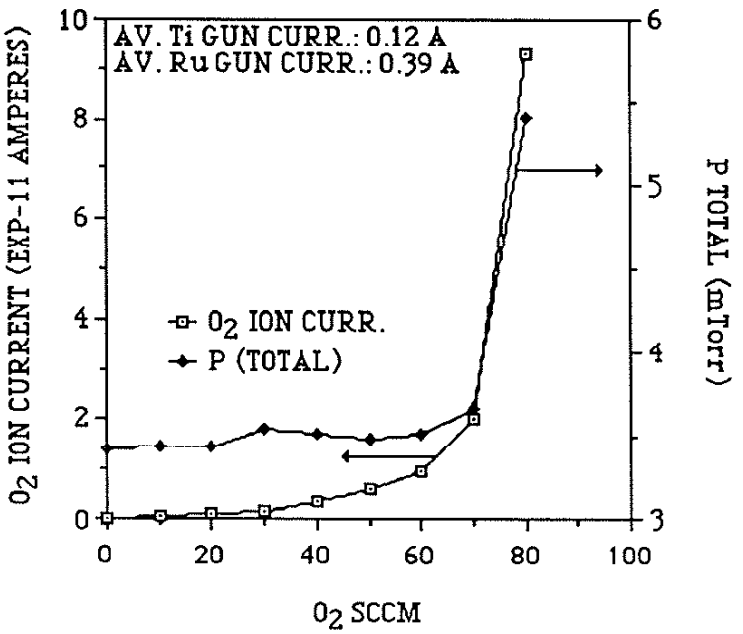

Figure 6. Oxygen consumption curve for reactive ion plated RuO_2 - TiO_2

Actual deposition runs commenced once a decision was made regarding the general processing window. The unannealed, machined niobium substrates were initially ground to a surface finish equivalent to that given by 600 grit silicon carbide abrasive paper. The niobium discs were then immersed in a room temperature acid solution for chemical polishing. Chemical polishing was chosen over further mechanical polishing because of the impracticality associated with mechanically polishing large field specimen substrates. The acid solution itself was a mixture of concentrated hydrofluoric (HF), nitric (HNO_3), and hydrochloric (HCl) acids in the following proportions:

15 ml HF
30 ml HNO_3
30 ml HCl
30 ml deionized H_2O.

The time duration of immersion of the niobium discs in the room temperature acid solution was three minutes. At the end of the polishing period the substrates were washed in deionized H_2O to dilute and remove any residual acid solution and were then placed into an acetone bath for ultrasonic cleaning.

Cleaned substrates were affixed to the cathode using RTO coated hardware. Fresh medical gloves and clean tweezers were always used to preserve surface cleanliness and reduce the time necessary for adequate evacuation of the chamber. Upon mounting the substrates and loading the ruthenium and titanium sources, the pump down sequence was initiated. During the pump down process the RGA was engaged, the liquid nitrogen traps atop the diffusion pumps were filled, and the gas conduits were opened and evacuated. Once base pressure was achieved, purging of the gas lines commenced and was monitored by observing the decline of contaminants within the upper chamber via the RGA. The purging process was followed by the introduction of argon whose flow rate was adjusted to correspond to an upper chamber pressure of 3 mTorr. Sputter cleaning of the substrates ensued with an RF generated argon glow discharge. The electron beam guns were engaged five minutes prior to the end of the sputter cleaning process to slowly and uniformly warm the ruthenium and titanium sources to their respective vaporization temperatures. Both the electron beam guns and the oxygen gas were increased to their desired levels concurrently at the start of the deposition. Continuous monitoring of the oxygen signal, given by the RGA, for data pertaining to the reactivity of oxygen with the ruthenium and titanium vapors occurred throughout the run. The electron beam guns were disengaged, the glow discharge extinguished, and the gas lines closed at the end of the run. The chamber was allowed to cool to approximately 40°C before opening and removing substrates. Once the substrates were removed or exchanged the chamber was again evacuated for the purpose of minimizing the adsorption of water molecules on its inner wall.

IV. ANALYTICAL PROCEDURE

A. ELECTRON MICROSCOPY

Both scanning and transmission electron microscopy (SEM and TEM, respectively) were employed to study the microstructure and morphology of the deposited oxide films. Scanning electron micrographs were taken using the Hitachi S-800 field emission scanning electron microscope located at the University of Illinois' Center for Microanalysis of Materials (UICMM). All of the scanning electron micrographs are of tensile fracture surfaces of RTO films deposited onto Corning 7059 borosilicate glass substrates. Film morphology, density, and thickness were analyzed from data obtained via the SEM. Information pertaining to microstructure, elemental chemistry, and phases present before and after anodic polarization (which is discussed in a later section) was obtained via the TEM. The TEM used in this study was a Phillips EM400T analytical electron microscope equipped with an EDAX 9100 energy dispersive spectroscopy (EDS) unit located at the UICMM. An attempt was made to determine, through the use of selected area electron diffraction on broad-face specimens, the identity of the oxide phases present and whether they were segregated or finely dispersed throughout the film. A goal of this phase of the study was to identify any structural and chemical changes occurring to the films as a result of their subjection to anodic polarization testing.

B. CHEMICAL AND PHASE ANALYSIS

In addition to the use of selected area electron diffraction in the TEM, phase analyses were also conducted with the Rigaku D-MAX x-ray diffractometer located at the UICMM. While there is little question that electron diffraction is the more sensitive of the two techniques, having the ability to provide detailed phase and

crystallographic information on specific grains within a prepared foil, x-ray diffraction can yield phase and orientation data over greater areas and depths and requires virtually no sample preparation. X-ray diffraction is a useful technique to obtain general phase information quickly and with minimal effort.

Quantitative elemental analyses were performed on all the oxide films using a JEOL JXA 50A Electron Probe Microanalyzer equipped with light optics and a Tracor Northern TN4000 X-ray Analyzer. With this technique it was possible to determine the relative atomic percents of ruthenium and titanium (as well as argon and other trace elements) incorporated into the coatings. The microprobe data was also correlated to the ruthenium and titanium evaporation rates as a function of electron beam gun current. EDS was used as a semi-quantitative verification of the electron microprobe results.

Surface chemical analysis was conducted by Auger electron spectroscopy (AES) using the Perkin Elmer PHI 660 Scanning Auger Multiprobe in an effort to determine whether or not failure of the oxide films under anodic polarization was the result of the loss, through dissolution or oxidation, of one or more of the coating constituents. Comparisons of the Auger surface profiles of pristine (unpolarized) and polarized films with the aid of quantitative elemental data provided by a multiplex operation was used to identify differences in elemental content.

Samples of the fresh water electrolyte used during anodic polarization testing were analyzed for their ruthenium, titanium, and niobium concentrations by inductively coupled argon plasma spectroscopy (ICAPS) at the Illinois Natural History Survey. The analysis was performed with a Jarrell-Ash Model 975 AtomComp Spectrometer. ICAPS data was used in conjunction with AES data to define the mechanism(s) of film failure.

C. FILM ACTIVITY TESTING

Recalling that it is desirable for mixed metal oxide films to have low electrical resistivities, sheet resistances were measured by the four point probe technique using a Kulicke & Soffa Industries Model 4640 Four Point Probe on films deposited onto Corning 7059 glass substrates. By combining film thickness data with the sheet resistance measurements it was possible to calculate film resistivity.

Anodic polarization of the oxide films at a high current density was employed to determine their activity, i.e. their electrochemical behavior, under accelerated conditions. The objective of activity testing is to identify those MMO films having the ability to maintain a stable flow of current with little or no rise in applied potential for extended time periods. The testing was performed using an EG&G Princeton Applied Research Model 173 Potentiostat/Galvanostat equipped with a Model 373 Current Converter. The potentiostat was operated in its galvanostatic mode to serve as a constant current source. Activity data was acquired by monitoring the time change in the potential difference between two graphite cathodic electrodes and a MMO anodic electrode, the latter being forced to maintain a constant flow of current. Only MMO films deposited onto niobium substrates were tested, and all specimens were subjected to a current density of 150 A/m^2; typical current densities encountered in impressed current cathodic protection systems are on the order of 25 A/m^2. Each of the films was tested in a fresh tap water electrolyte.

V. RESULTS AND DISCUSSION

A. PROCESSING AND SPECIMEN PARAMETERS

Table 1 lists the significant ion plating processing parameters chosen for the fabrication of RTO films on niobium and Corning 7059 borosilicate glass substrates. Recall that the consumption curve generated for the RuO_2 - TiO_2 system (Figure 6) exhibited a knee at approximately 70 sccm, the point at which reactivity between oxygen gas and the ruthenium and titanium source materials is at its optimum. Note from Table 1 that series A films were fabricated using an average oxygen flow rate below that of the knee of the consumption curve. Quantitative elemental analysis of series A films via the electron microprobe shows them containing approximately 85 at.% titanium and 15 at.% ruthenium (Table 2). Yet ruthenium, in neither its elemental or oxide phases, appears in the film's x-ray diffraction pattern (Figure 7). Instead, the diffraction pattern reveals only the presence of TiO_2 (rutile). The sole presence of TiO_2 (rutile) diffraction peaks, together with microprobe data verifying ruthenium as a film constituent, indicates that the ruthenium is incorporated into the film in solid solution. A MMO film comprised of TiO_2 (rutile) and ruthenium in solid solution is plausible. Consider first that the Hume-Rothery rules for substitutional solid solution are applicable and satisfied. Secondly, a Mossbauer spectroscopy study performed by Triggs et. al. [28] on single crystal TiO_2 containing 2 at.% ruthenium concluded that ruthenium can in fact replace titanium substitutionally in TiO_2 as Ru^{4+}. In addition, Roginskaya et. al. [9], focussing on the electrical transport properties of the RuO_2 - TiO_2 system, concluded that Ru^{3+} as well as Ru^{4+} ions replace Ti^{4+} in TiO_2. Finally consider that the heat of formation of TiO_2 (rutile) is -228,360 g•cal/mol and that the heat of formation for RuO_2 is -57,290 g•cal/mol [29]. Of these two oxides, the formation of TiO_2 is, therefore, the most favorable. Given that the oxygen flow rate is below the knee of the RuO_2 - TiO_2 consumption curve it is likely that titanium getters all available oxygen when forming its oxide. The

ruthenium source is then left with an insufficient amount of oxygen with which to react and is thus incorporated into the film in substitutional solid solution.

The average oxygen flow rate was increased to approximately 73.5 sccm when fabricating series B MMO films. The result, given in Table 2, was a TiO (cubic) film with ruthenium in solid solution. This was an interesting and initially perplexing result because TiO_2, and not TiO, is the thermodynamically stable oxide phase of titanium [30]. The presence of ruthenium in the series B MMO films was verified by both electron microprobe analysis and EDS in the TEM; the mean atomic percentages of titanium and ruthenium are listed in Table 2. Selected area electron diffraction of a series B TEM specimen clearly shows that the MMO film has a TiO (cubic) crystal structure and, as with the series A films, contains no elemental or oxide phase of ruthenium (Figure 8, Table 3). The heat of formation of TiO is roughly -125,010 g•cal/mol and it, like its TiO_2 counterpart, should form preferentially over RuO_2. Thus the ruthenium is incorporated into the film in solid solution. The formation of TiO can possibly be explained given the following premise. Upon concluding series A deposition, the flow of oxygen gas to the ion plating chamber was intentionally continued to monitor and document total chamber pressure as power to the glow discharge and electron beam guns was decreased. Concurrently, the ruthenium and titanium sources were beginning to cool; at this point in time the source temperatures were just below their respective melting temperatures. The titanium source was positioned such that it lay in the path of oxygen flow. If the titanium source was poisoned by residual oxygen during the time the compact (and vacuum chamber) was cooling, a small percent of the source's surface could have oxidized and formed TiO_2.

Table 1 - Processing Parameters

Specimen Series	Average Pressure	Average O_2 Flow Rate	Ti Gun Current	Ru Gun Current	Average Deposition Rate
A	0.50 Pa	61.1 sccm	0.11 A	0.40 A	0.633 nm/s
B	0.47 Pa	73.5 sccm	0.14 A	0.41 A	1.46 nm/s
C	0.48 Pa	95.5 sccm	0.13 A	0.39 A	0.872 nm/s
D	0.62 Pa	97.1 sccm	0.15 A	0.40 A	1.02 nm/s
E	0.61 Pa	100 sccm	0.15 A	0.35 A	1.09 nm/s
F	0.69 Pa	96.7 sccm	0.15 A	0.32 A	1.40 nm/s
G	0.64 Pa	96.4 sccm	0.15 A	0.32 A	1.24 nm/s

Constant Parameters
Power Density: 3.3 W/cm^2
Deposition Time: 30 min.
Maximum Deposition Temperature: 400°C

Table 2 - Specimen Parameters

Specimen Series	Film Thickness	Resistivity (Ω-cm)	Decrease in Film Activity	Mean at.% Ti	Mean at.% Ru	Chemistry/Phases Present *
A	1.14 μm	$3.220 \cdot 10^{-1}$	yes	85	15	TiO_2 (R) with Ru in soln.
B	2.63 μm	$2.719 \cdot 10^{-3}$	yes	87.5	12.5	TiO (cubic) with Ru in soln.
C	1.57 μm	5.423	no	90	10	TiO_2 (R) & RuO_2
D	1.83 μm	$2.375 \cdot 10^{-3}$	yes	52	48	TiO_2 (R) & RuO_2
E	1.97 μm	$1.156 \cdot 10^{-1}$	no	80.5	19.5	TiO_2 (R) & RuO_2
F	2.53 μm	112.5	yes	95	5	TiO_2 (A+R) & RuO_2
G	2.23 μm	beyond measuring capability	yes	97.5	2.5	TiO_2 (A+R) & RuO_2

* A = anatase
R = rutile

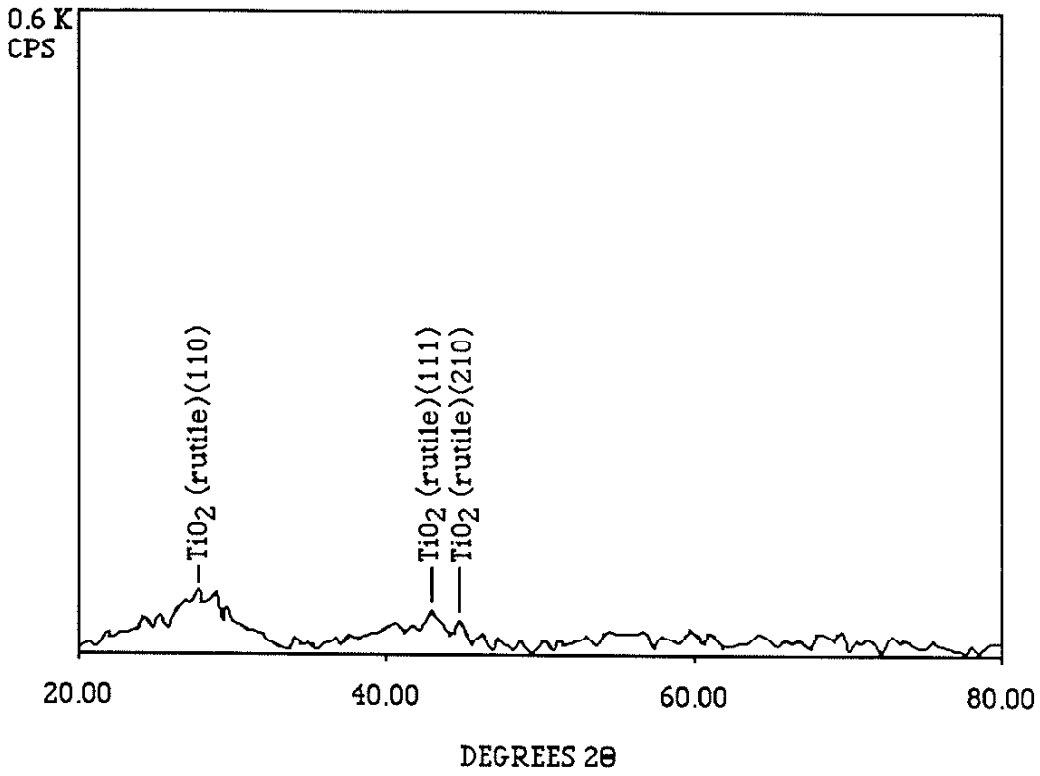

Figure 7. X-ray diffraction 2θ scan of series A films showing the presence of TiO_2 (rutile) diffraction peaks

According to Maissel and Glang [31], electron beam evaporation of oxide compounds like TiO_2 is accompanied by incongruent evaporation, i.e. the compound dissociates into constituents which do not volatilize at equal rates. The vapor species observed (listed in order of decreasing frequency) during the electron beam evaporation of TiO_2 are TiO, Ti, TiO_2, and O_2. The presence of a TiO film is not so surprising given a starting source material containing a significant amount of TiO_2 at its surface.

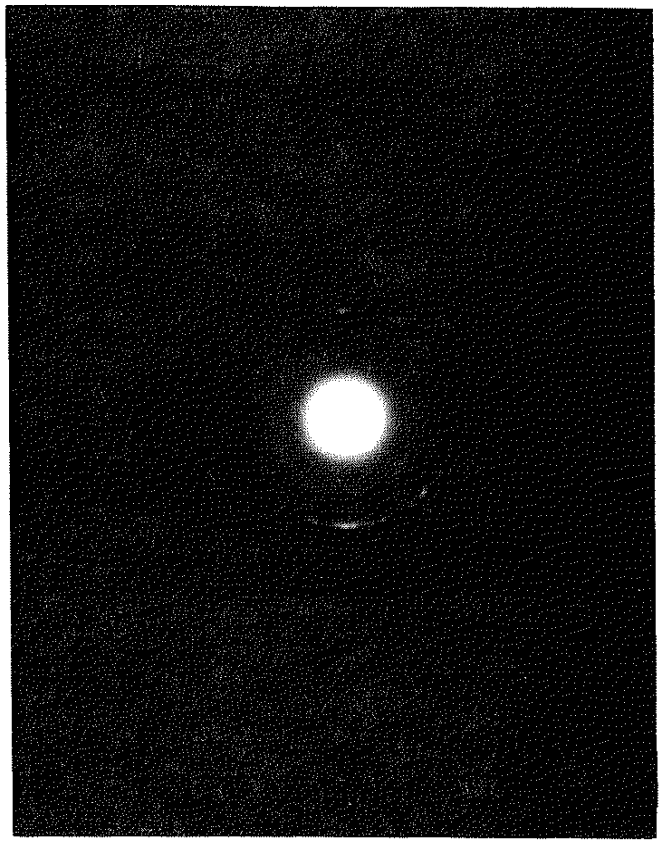

Figure 8. Selected area electron diffraction pattern of series B MMO films showing the ring pattern of a polycrystalline TiO (cubic) phase

Table 3 - TiO (series B) electron diffraction pattern analysis

Ring Number	Crystallographic Plane
1	TiO (111)
2	TiO (200)
3	TiO (220)
4	TiO (222)
5	TiO (420)
6	TiO (422)

Series C, D, and E films, each comprised of different titanium and ruthenium contents (Table 2), consist of what can be adequately described as a dual phase mixture of RuO_2 and TiO_2 phases. Peak splitting evident in x-ray diffraction 2θ scans (Figure 9) from series C, D, and E films is generally not observed for RuO_2 - TiO_2 films processed at temperatures below 650°C via conventional solidification techniques. Oxide annealing temperatures for MMO films deposited via thermal decomposition are intentionally kept below 650°C to minimize sintering effects. Sintering MMO films often leads to cracking which may serve to expose the substrate to an electrolyte thereby increasing the probability of deleterious chemical reactions and subsequent substrate dissolution [32]. The absence of distinct RuO_2 and TiO_2 (rutile) phases in most MMO films fabricated via thermal decomposition methods can be attributed to these lower processing temperatures. The high temperature microstructures of the series C, D, and E films are effected by the ion plating deposition technique. Note that the high temperature RuO_2 - TiO_2 (rutile) microstructures were produced at relatively low deposition temperatures without inducing the cracking associated with high temperature sintering. Experimental data from this study, which is presented in a subsequent section of the text, shows that a film comprised of a combination of RuO_2 and TiO_2 (rutile) phases is

desirable in an impressed current MMO anode. The average oxygen flow rates used to process series C, D, and E films were well above the knee of the RuO_2 - TiO_2 consumption curve. The formation of RuO_2 is attributed to the relatively high oxygen partial pressure within the deposition chamber. The RuO_2 - TiO_2 (rutile) combination formed only when the average oxygen flow rates exceeded 95 sccm (Table 1). It is interesting to note that as the atomic percentage of titanium is increased for each of the RuO_2 - TiO_2 films it is accompanied by a corresponding increase in film resistivity (Table 2). The observed increases in film resistivity with increasing titanium content are in good agreement with results reported by Hine et. al. [11].

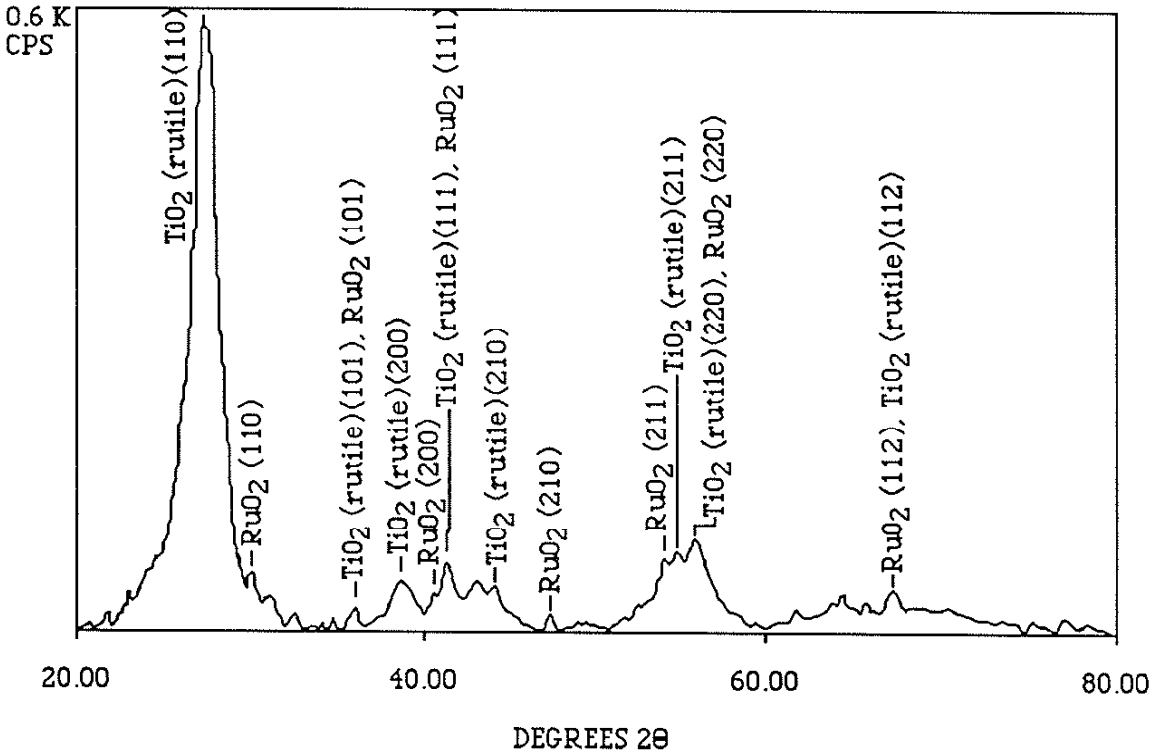

Figure 9. X-ray 2θ scan of a series C film (also representative of D and E films) showing overlapping and separate RuO_2 and TiO_2 (rutile) diffraction peaks

Series F and G films are MMO coatings containing less than 10 at.% ruthenium while retaining the RuO_2 - TiO_2 (rutile) crystal structure. X-ray diffraction 2θ scans of series F and G films (Figure 10) vividly show the presence of TiO_2 (anatase) in addition to RuO_2 and TiO_2 (rutile) diffraction peaks. The presence of TiO_2 (anatase), based on processing conditions used to fabricate series F and G films, may be related to the intentional decrease in ruthenium evaporation rates which lead to corresponding decreases in elemental ruthenium content (Tables 1 and 2). The remaining variable process parameters (Table 1) were kept virtually unchanged with respect to the deposition conditions employed in the fabrication of series C, D, and E films. The decreased ruthenium content obviously lowers the percentage of RuO_2 within the films. Recall Gerrard and Steele [13] concluded that 5-10 mol% $RuCl_3$ was responsible for stabilizing the TiO_2 (rutile) structure in RuO_2 - TiO_2 films. It is possible that a finite percentage of RuO_2, which has the same crystal structure as TiO_2 (rutile) and a similar lattice parameter, is necessary to stabilize TiO_2 (rutile), and that an elemental ruthenium content of less than 10 at.% is insufficient in providing this required percentage of RuO_2. The effect of lowering the RuO_2 content in the series F and G films is also manifested in high resistivity readings obtained for these films via the four point probe (Table 2); recall that RuO_2, a metallic conductor, contributes heavily to the conductivity of RTO films.

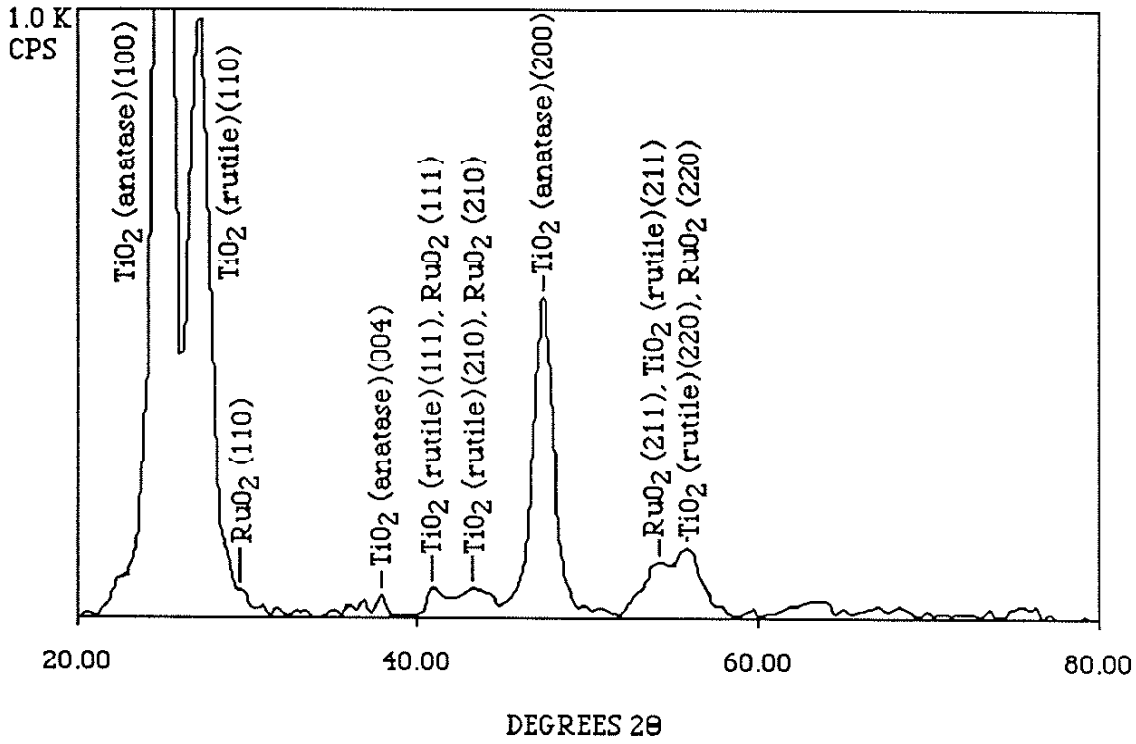

Figure 10. X-ray 2θ scan of a series G film (also representative of the F films) showing the presence of TiO_2 (anatase) in addition to RuO_2 and TiO_2 (rutile) phases

B. ELECTRON MICROSCOPY

Scanning electron micrographs of tensile fracture surfaces provide data pertaining to film morphology, density, and thickness (thickness data is listed in Table 2). Differences in morphology, density and thickness associated with ion plated films are a function of a combination of many paramcters including substrate surface roughness, substrate temperature during deposition, deposition rate, gas pressure, and the angle of incidence of the evaporant flux [21]. The structure zone model developed by Thornton [33] attempts to account for morphological variations resulting from differences in substrate surface temperature with respect to the melting

temperature of the source material, as well as changes in argon gas pressure. The approach, however, does not account for many other important parameters affecting the nature of ion plated film growth, such as the role of adatom mobility, to be of great use in relating morphological features to specific processing conditions.

Figures 11, 12, and 13 are scanning electron micrographs of series A, C, and G films, respectively. Each of these MMO coatings exhibits a zone 1 morphology as described by Thornton's structure zone model, i.e. all three MMO films have a distinctive columnar morphology with dome-shaped apexes. The roughened surface created by the dome-shaped column apexes, shown best in Figure 13, is a desirable feature for a MMO anode coating because it serves to increase the anode's effective surface area thereby enhancing electrochemical activity and decreasing film resistance [5]. The anode films appear to be very dense. The morphological features depicted in Figures 11-13 are representative of the remaining ion plated MMO films on niobium and Corning 7059 borosilicate glass with the exception of the series B films. Figure 14 is a scanning electron micrograph of a series B film. While the film has a columnar morphology with dome-shaped column apexes at the surface, it does not exhibit the same zone 1 morphology which typifies the remaining series of MMO films produced for this study. Rather, the series B films contain morphological features similar to those described by the Thornton structure zone model for coatings with a zone T morphology. A Zone T (T for transition) morphology is characterized by a dense array of poorly defined fibrous, columnar grains. The columnar grains in the series B film are not aligned perpendicularly to the plane of the substrate. The film appears to be very dense. Recall that Triggs' [10] SEM analysis of RuO_2 - TiO_2 single crystals fabricated via chemical vapor deposition found directional alignment of a white platelet ruthenium-rich phase. Evidence of a platelet structure, or directionality, was not observed in the ion plated, polycrystalline MMO's fabricated for this study.

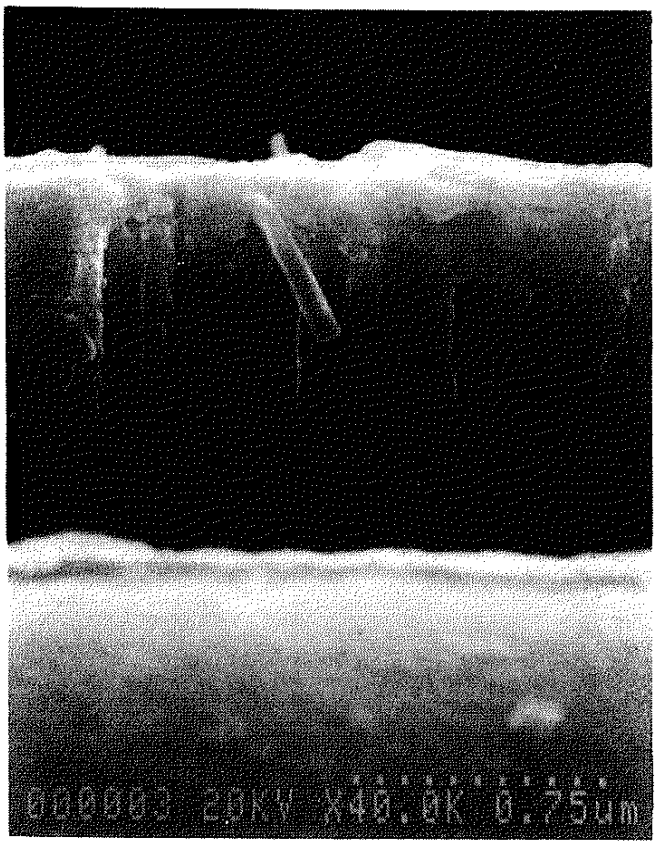

Figure 11. Scanning electron micrograph of a series A fracture specimen exhibiting a zone 1 columnar morphology

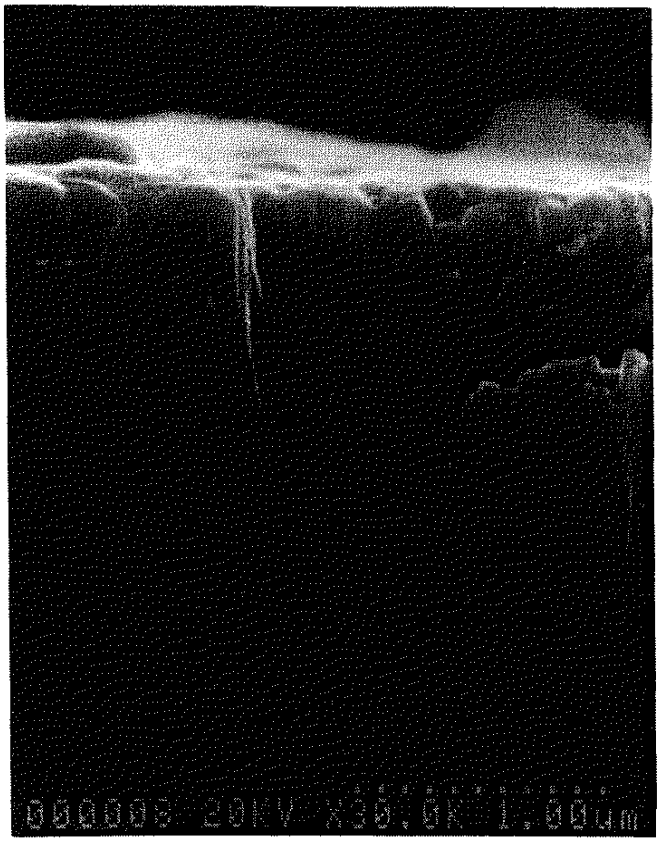

Figure 12. Scanning electron micrograph of a series C fracture specimen exhibiting a zone 1 columnar morphology

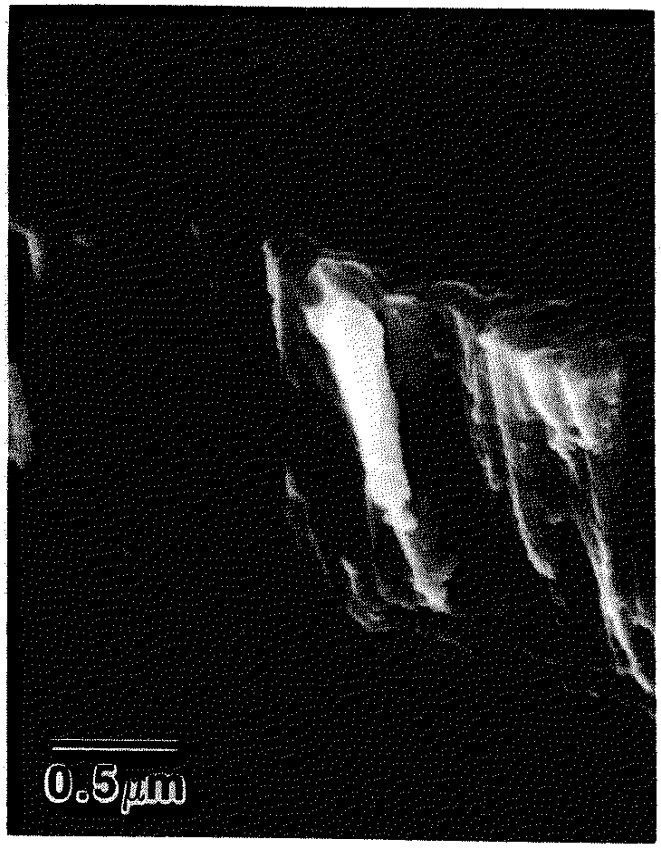

Figure 13. Scanning electron micrograph of a series G fracture specimen exhibiting a zone 1 columnar morphology

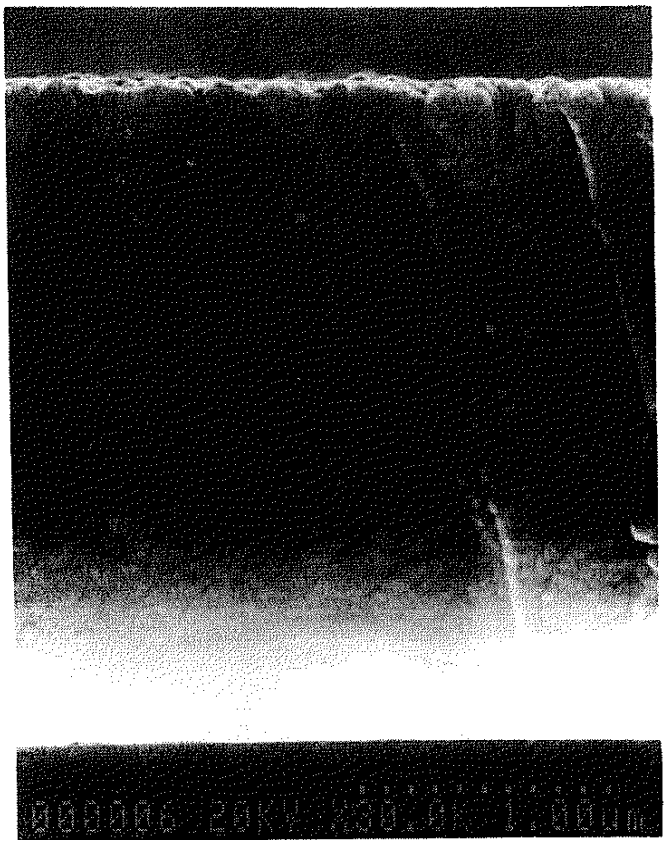

Figure 14. Scanning electron micrograph of a series B fracture specimen exhibiting a zone T columnar morphology

Microstructure and chemical compositions of crystalline phases within the ion plated MMO films were examined with transmission electron microscopy. One of the goals of this phase of the study was to identify those grains, or areas within a grain, containing either RuO_2 and/or TiO_2, and to determine whether or not the RuO_2 and TiO_2 phases were segregated or finely dispersed throughout the deposited film. Figure 15 is a broad-face bright field transmission electron micrograph of a series G film. The structural features within this micrograph are illustrative of those found in series A-G films. Moire fringes, visible within the planar sections of individual columns (these are similar to the columns seen in the SEM fracture specimens), are indicative of overlapping grains. The columns are, therefore, not comprised of single crystals. The concentric rings which make up the selected area electron diffraction pattern of a series G film (Figure 16) also indicate that its microstructure is polycrystalline and randomly oriented (at least within the plane of the film). Though each of the MMO films characterized with the SEM appeared to be very dense, porosity at the boundaries of the individual columns is evident in the transmission electron micrograph of Figure 15. The porous structure, however, may not penetrate much below the top surface of the film. The fact that the G series specimen is a broad-face TEM foil (as were the other TEM specimens used in this study) which was milled from its bottom (substrate) side and, recalling from the scanning electron micrographs that the column apexes are rounded at the film's upper surface, Figure 15 likely represents only the top surface region of the deposited film. The extent of porosity, therefore, may not be great. The actual degree of porosity will be determined in future studies using cross-section TEM (XTEM). It is important to ascertain the degree of porosity of any MMO film used as an impressed current anode because of the detrimental effect interconnected pores can have on substrate oxidation and subsequent dissolution.

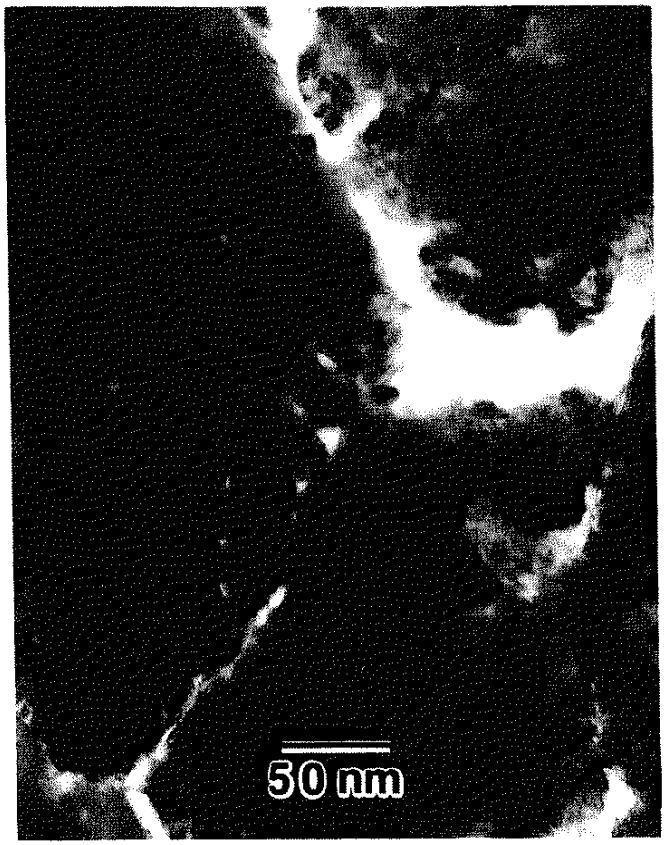

Figure 15. Bright field transmission electron micrograph of a series G film showing Moire fringes and porosity at column boundaries

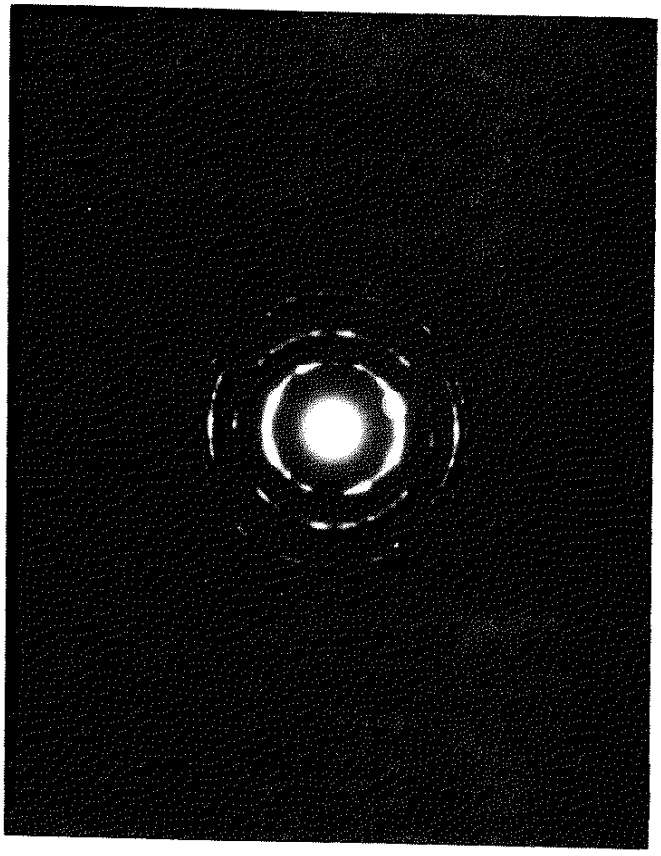

Figure 16. Selected area electron diffraction pattern of a series G film

Figure 17 is a dark field TEM image of the same area on the series G film that was used to form the bright field TEM image depicted in Figure 15. The dark field image was derived from the first ring of the selected area electron diffraction pattern given in Figure 16. This diffraction ring, which is clearly marked by the TEM's objective aperture, corresponds to the {101} reflection of TiO_2 (anatase). The bright regions of the dark field image depicted in Figure 17 correspond to multiple TiO_2 (anatase) crystals. Because of the diffuse and overlapping nature of most of the film's diffraction rings, it was not possible to image, in the dark field condition, all regions of the columns to identify them as being either RuO_2 or TiO_2-rich. Due to numerous overlapping and diffuse diffraction spots generated from a multitude of diffracting microcrystals, no additional information was obtained through a conventional microdiffraction technique. Scanning transmission electron microscopy (STEM), by virtue of its small probe size (≈5 nm in diameter), could provide a sensitive point chemical/phase analysis yielding the data necessary to determine the degree of homogeneity or inhomogeneity of the RuO_2 dispersion within the MMO film. Such an analysis will be performed in the future on this system.

Figure 17. Dark field transmission electron micrograph of a series G film showing TiO_2 (anatase) crystals

C ANODE ACTIVITY TESTING

The activity test, as described by Loucka [34], was used to determine the electrochemical behavior of anodically polarized MMO films. As was previously stated, the objective of such a test is to identify those MMO films possessing the ability to maintain a stable flow of current while anodically polarized, and which concurrently show little or no rise in applied potential for extended time periods. MMO films (deposited onto valve metal substrates) possessing such characteristics are ideal for use as impressed current cathodic protection anodes.

Figure 18, an activity plot of a series A film, depicts the almost linear increase in voltage with respect to time which was required to sustain a current density of 150 A/m^2. While the potential increase was only 5 volts, activity testing was discontinued due to the film's rapid physical deterioration which indicated imminent failure. Failure refers to the MMO film's inability to continue to support a constant flow of current with an applied potential of 85 volts or less. The 85 volt limit was chosen for two reasons. First, an impressed current cathodic protection anode operating at, or above 85 volts is not an economically feasible device. Second, potential measurements above 85 volts approached the output limit of the potentiostat/galvanostat used in this study. Figures 19 and 20 show the series A film's physical transition from the pristine to polarized (and deteriorated) condition. Note that the progression of film deterioration was radial, i.e. degradation first occurred at the coating edge and then continued toward the center of the niobium-coated disc. The mode of failure may be due to the fact that higher current densities exist at the edge of the coated disc, however, other films subjected to identical test conditions did not deteriorate in the same manner. Comparisons of Auger surface surveys of pristine and anodically polarized series A films show a decrease in ruthenium content from the pristine to polarized condition. In addition, the surface surveys show the emergence of niobium in the polarized films; niobium is absent in surface surveys of pristine films. These

Auger results suggest that the mechanism(s) of film failure, and loss of electrochemical activity, may be due to a combination of ruthenium loss and substrate oxidation. An Auger surface survey of a series A film in its pristine condition is given in Figure 21. A subsequent Auger surface survey of the remaining coated area of a polarized series A film shows a marked decrease in the film's ruthenium content and virtually no change in its titanium content (Figure 22). A third Auger surface survey (Figure 23), detailing the chemical content of the delaminated, exposed region of the niobium coated disc (shown in Figure 20), indicates that the series A film experienced virtually total dissolution in that region and was supplanted by the formation of a niobium oxide film. It is likely that onset of the series A failure was caused by the initial depletion of its ruthenium component.

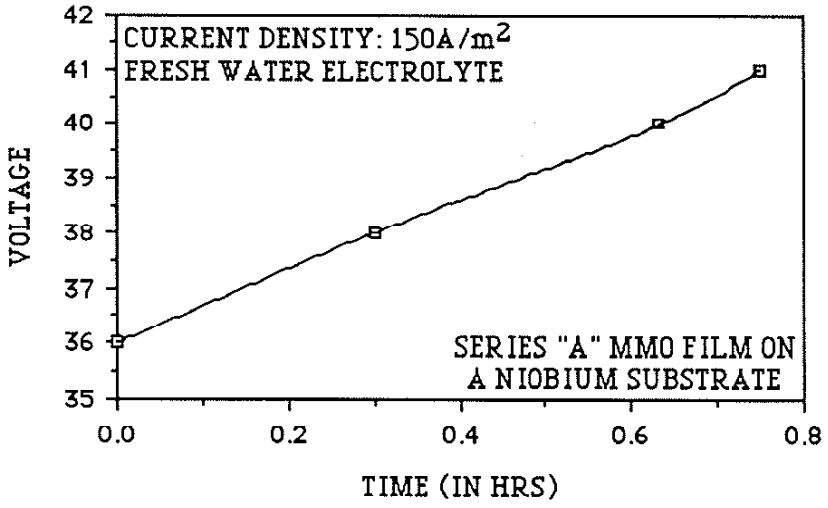

Figure 18. Activity plot of a series A film showing the linear increase in applied potential with time which was necessary to sustain a current density of 150 A/m^2

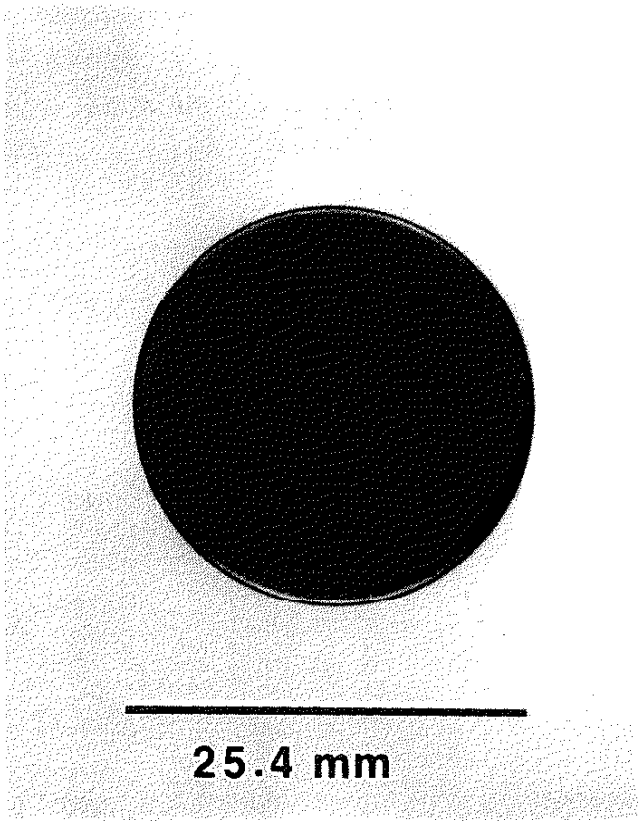

Figure 19. Photograph of a pristine film deposited onto a niobium substrate

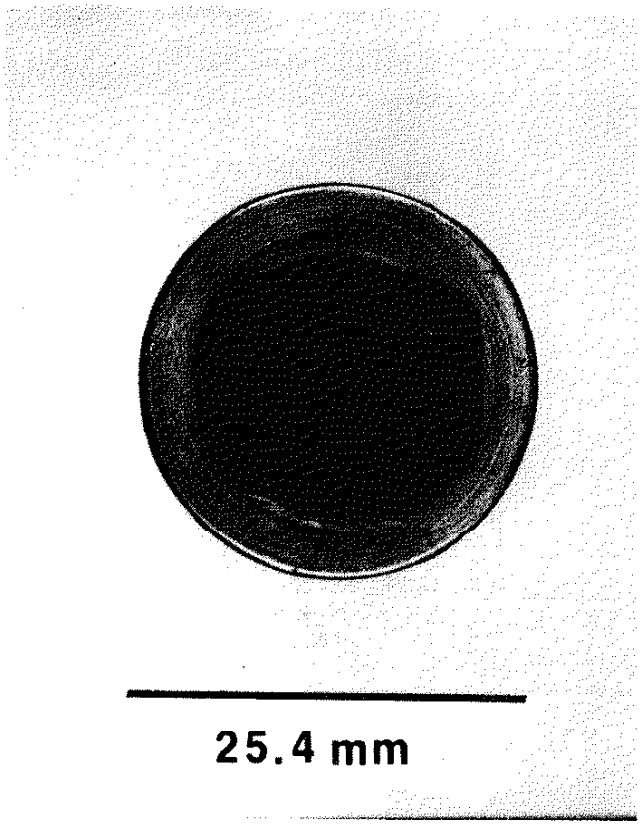

Figure 20. Photograph of an anodically polarized series A film showing coating dissolution initiated at the disc edge

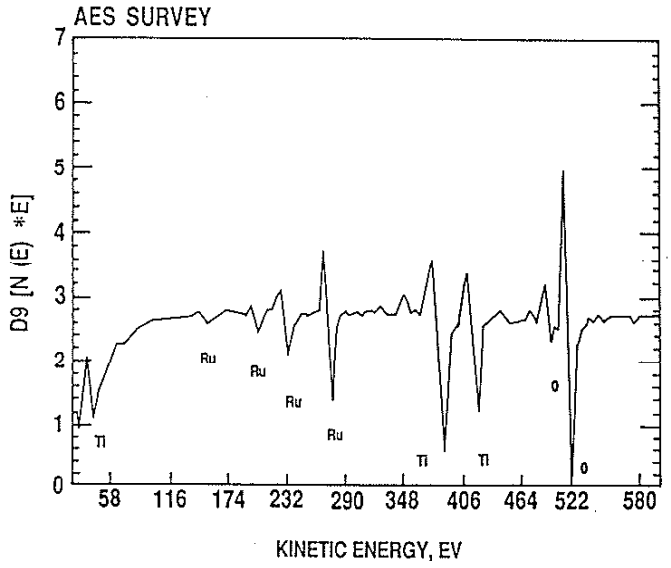

Figure 21. Auger Surface survey of a pristine series A film

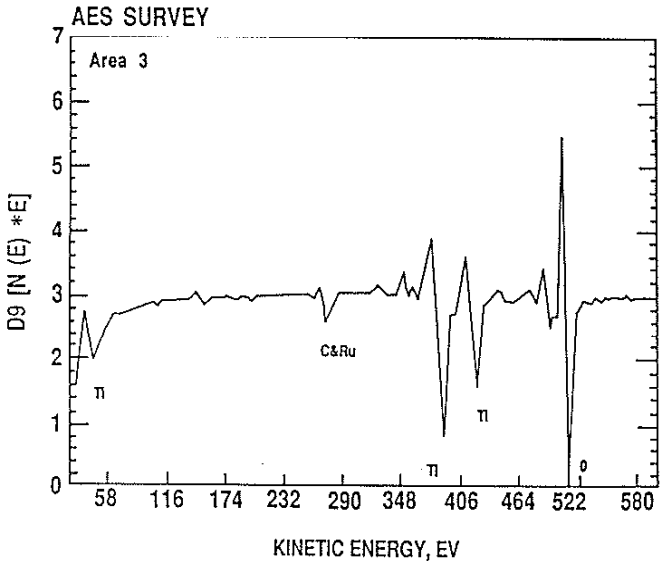

Figure 22. Auger surface survey of the remaining coated area on a polarized series A film (Refer to Figure 20); note the decrease in height of the ruthenium peaks indicating Ru loss

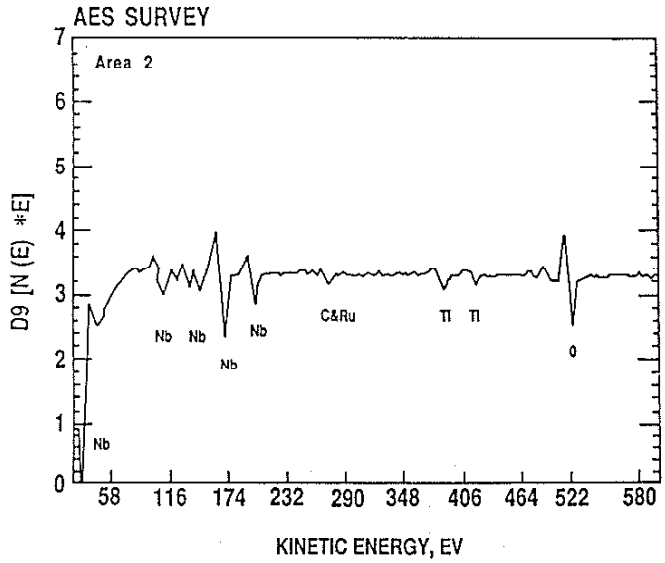

Figure 23. Auger surface survey of the exposed (uncoated) region of a polarized series A film (refer to Figure 20); note the emergence of niobium

While the mode of failure differed, the mechanism by which series B films failed was similar to that described for series A. Comparative Auger surface surveys of pristine and polarized series B films show a marked decrease in ruthenium content. The physical deterioration of polarized series B films was distinguished by uniform film spalling (Figure 24), and substrate oxidation. A series B activity plot, depicted in Figure 25, is very similar to activity plots generated from electrodes forming non-conducting, surface oxide films [11]. Though an electrically insulating niobium oxide surface film did form on the series B substrate, its formation was concurrent with, or preceded by a substantial loss of ruthenium from the deposited film.

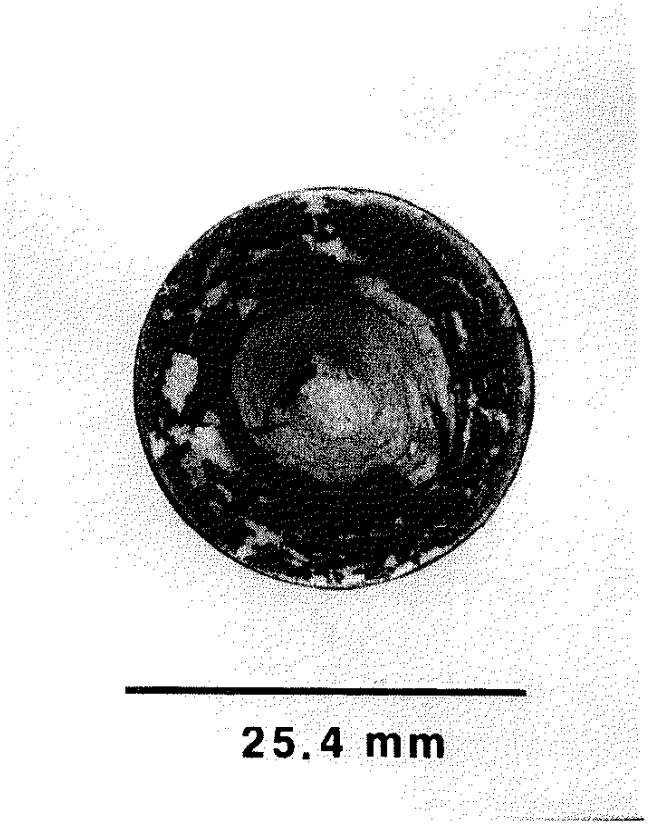

Figure 24. Photograph of a polarized series B film showing film spalling

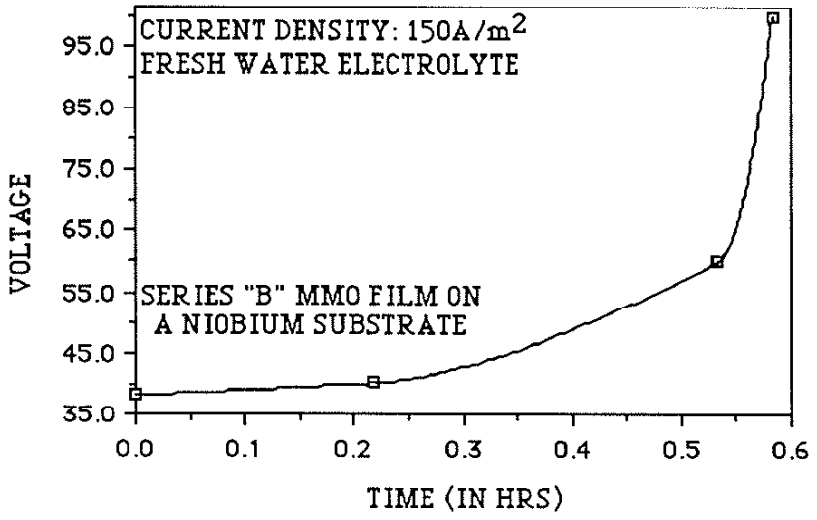

Figure 25. Activity plot of a series B film showing a rapid increase in applied potential with time to sustain a current density of 150 A/m^2

Series C, D, and E films displayed the greatest longevity of those tested. Of the three, series C and E best resisted the coating degradation and electrochemical loss associated with extreme anodic polarization. Figure 26 is an activity plot of a series E film; series E activity plots were similar to those generated by series C films. Note that the initial voltage readings generated by the series E film under anodic polarization (as well as those generated by series D, F, and G) are approximately 35% greater than those reported for series A and B. The potential increase is directly related to a corresponding 35% decrease in the film surface area exposed to the electrolyte. The original test fixture in which the niobium coated discs were mounted was damaged and replaced with a second fixture whose dimensions decreased the surface area of the film exposed to the electrolyte by roughly 35%. Apart from an initial rise in applied potential at the onset of polarization, no increases in voltage were required by either series C or E films to maintain a constant flow of current over an extended period of time. Activity testing of the series C and E films

was discontinued after 75 hours and 76 hours, respectively, and was followed by chemical analysis via Auger microprobe and phase analysis via selected area electron diffraction. The physical and chemical integrity of both series of films was preserved throughout the duration of the activity test. Figures 27 and 28 are photographs of the pristine and polarized series C films. The discolored, slightly damaged outer ring at the edge of the coated niobium disk is due to the deterioration and removal of the gasket upon which the disk was seated while in its test fixture. Aside from blemishes associated with the substrate finish, the polarized film appears undamaged. Auger surface surveys performed on both series C and E films indicate that no loss of coating constituents occurred as a result of anodic polarization. Auger surface surveys of pristine and polarized series C films are given in Figures 29 and 30, respectively. Selected area electron diffraction of the polarized films showed that each series maintained the RuO_2 and TiO_2 (rutile) crystal structure through polarization testing (Figure 31, Table 4).

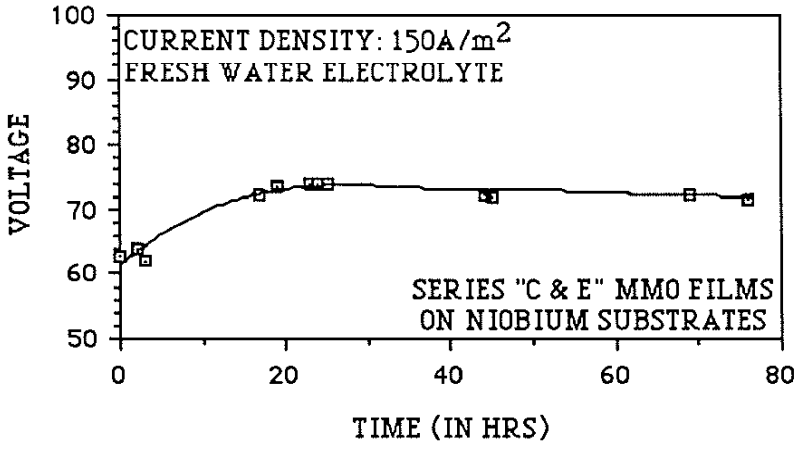

Figure 26. Activity plot of a series E film; aside from an initial increase in potential with time, little to no increase in voltage was required to maintain a current density of 150 A/m^2; series C activity plots were similar to those for series E

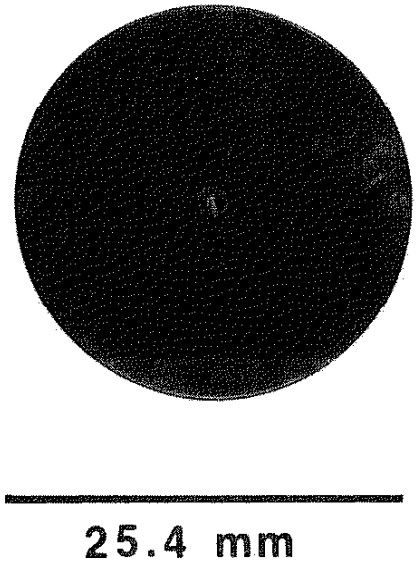

Figure 27. Photograph of a pristine series C film

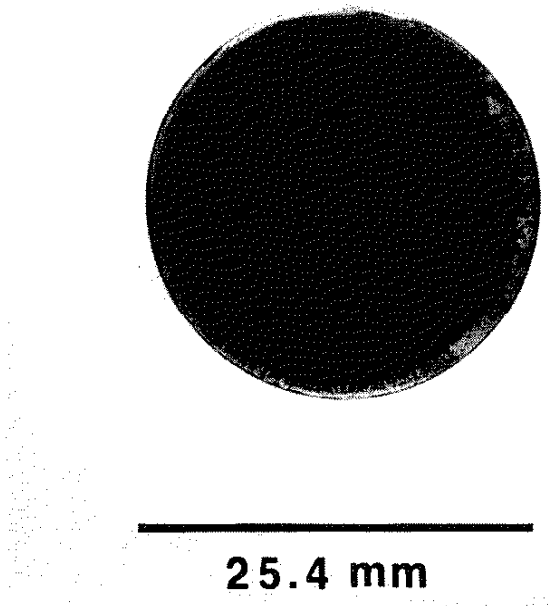

Figure 28. Photograph of a polarized series C film showing no loss of coating integrity from testing; polarized series E films appeared similar to the series C films

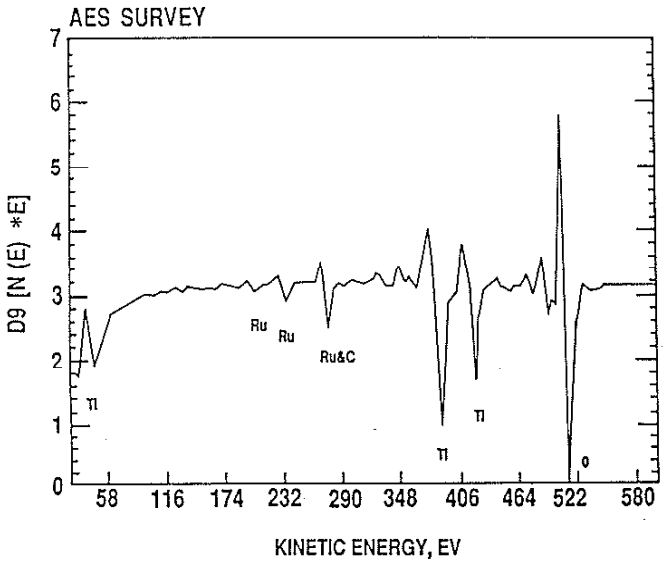

Figure 29. Auger surface survey of a pristine series C film

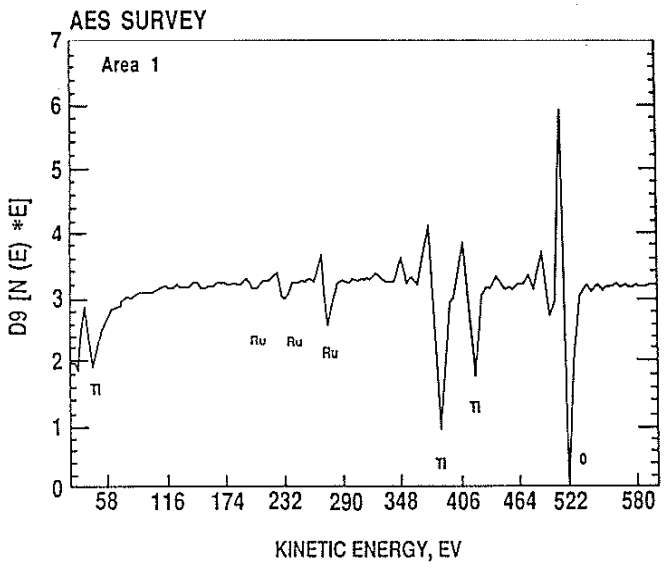

Figure 30. Auger surface survey of a polarized series C film; note that there is virtually no difference in elemental content between the pristine (Figure 29) and polarized films

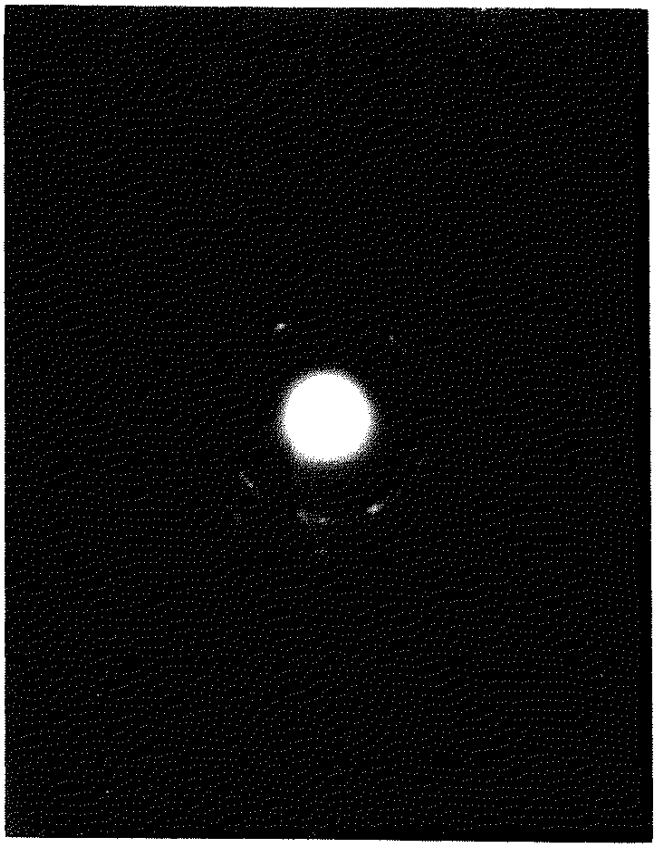

Figure 31. Selected area electron diffraction pattern of a polarized series E film showing that the film maintained its RuO_2 - TiO_2 phases throughout polarization testing; similar results were obtained for series C films

Table 4 - Series E selected area electron diffraction pattern analysis

Ring Number	Crystallographic Plane
1	TiO_2 (rutile)(110), RuO_2 (110)
2	TiO_2 (rutile)(101), RuO_2 (101)
3	TiO_2 (rutile)(111), RuO_2 (111)
4	TiO_2 (rutile)(210), RuO_2 (210)
5	TiO_2 (rutile)(211), RuO_2 (211)
6	TiO_2 (rutile)(310), RuO_2 (310)
7	TiO_2 (rutile)(301), RuO_2 (301)

Recall that series C films consist of approximately 90 at.% titanium and 10 at.% ruthenium, while series E films contain roughly 80.5 at.% titanium and 19.5 at.% ruthenium (Table 2). Series D films, while also possessing the RuO_2 - TiO_2 (rutile) crystal structure, are comprised of 52 at.% titanium and 48 at.% ruthenium. Failure of the series D films occurred within 24 hours from the onset of anodic polarization (Figure 32). No evidence of substrate spalling (from complete substrate oxidation) was apparent. The coatings exhibited a degree of discoloration following anodic polarization. Auger surface surveys performed on the pristine and polarized series D films show a decrease in their overall ruthenium content. This decrease was verified by ICAPS. Ruthenium was found in the series D electrolyte after polarization testing. Loss of electrochemical activity may be attributed to the loss of ruthenium. Though polarized series D films may retain as much ruthenium as is present in pristine, and successful, series C and E films, depletion of ruthenium in the series D films could have been accompanied by morphological changes which may have adversely affected film electrochemical behavior and performance. For example, a partial loss of ruthenium may have led to an increase in film porosity, or to the formation of an interconnected pore structure. Such an occurrence could lead to

electrolyte-substrate contact resulting in localized substrate passivation. The formation of electrically insulating niobium oxide films at various points along the coated disc would lead to an increase in the potential required to sustain the forced constant current flow. SEM analysis will be performed on both the polarized film surface and on fracture specimens to document any morphological changes which might have occurred during polarization.

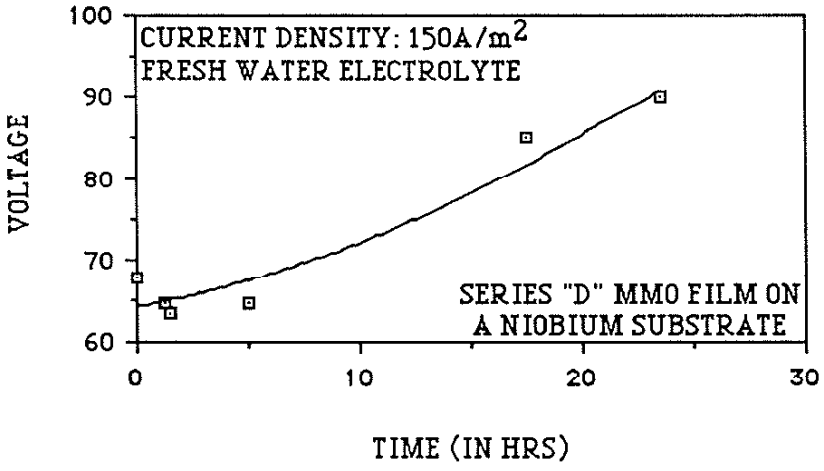

Figure 32. Activity plot of a series D film

It is evident that the RuO_2 - TiO_2 (rutile) composition is at least in part responsible for the success of the series C and E anode films under anodic polarization conditions. A processing window may exist between 80 at% titanium (20 at.% ruthenium) and 90 at.% titanium (10 at.% ruthenium) within which ion plated MMO films consisting of RuO_2 and TiO_2 (rutile) exhibit the necessary electrochemical properties required by impressed current cathodic protection anodes.

An activity plot for series F films is given in Figure 33; the electrochemical activity of series G films was similar to that of series F. Both series F and G films experienced a rapid rise in potential with time which was accompanied by film spalling; failure of series F and

G films occurred within 10 hours from the onset of polarization. While the presence of ruthenium in films from both series was verified by electron microprobe analysis (Table 2), and subsequently by EDS and selected area electron diffraction of TEM specimens (Figure 16 shows the presence of RuO_2), ruthenium was not detected in either the pristine or polarized films by the Auger microprobe. AES is a surface sensitive technique. If the ruthenium component was depleted at the film's surface, and should the depletion region extend to depths greater than 5 nm below the film's surface after sputtering, the element would not have been detected by an Auger surface survey. Auger depth profiling will be performed in future studies to determine the actual location of the ruthenium component. Without conclusive Auger data, the mechanism of failure cannot be definitively stated. Recall that the as-deposited series F and G films consisted of TiO_2 (anatase), RuO_2, and TiO_2 (rutile). Selected area electron diffraction of the polarized series F and G films (shown previously for a series G film in Figure 16) shows only the presence of RuO_2 and TiO_2 (anatase). It is likely that a phase transformation from TiO_2 (rutile) to TiO_2 (anatase) was induced under polarization conditions. This, or similar phenomena, has not been reported in the literature. Because of the lattice parameter mismatch between TiO_2 (anatase), TiO_2 (rutile) and RuO_2 (TiO_2 (anatase): $a_o = 3.78$, $c_o = 9.51$; TiO_2 (rutile): $a_o = 4.59$, $c_o = 2.96$; RuO_2: $a_o = 4.49$, $c_o = 3.10$), a titanium rutile-to-anatase phase transformation could effect film spalling. Film spalling may also have resulted from substrate oxidation. A full summary of activity test results for series A-G MMO films is given in Table 5.

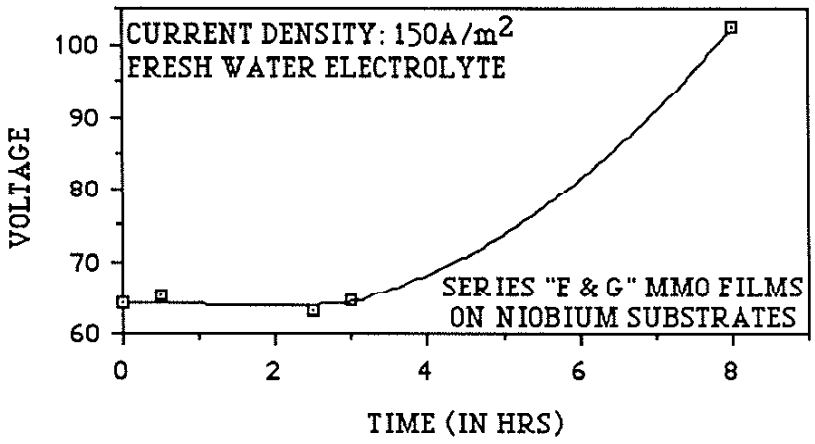

Figure 33. Activity plot of a series F film showing film failure in under 10 hours; series G films also exhibited this behavior

Table 5 - Summary of activity (anodic polarization) test data

Specimen Series	Time Duration of Anodic Polarization	Film Failure	Mechanism of Failure
A	0.75 hrs	imminent	Ru loss & substrate oxidation
B	0.58 hrs	yes	Ru loss & substrate oxidation
C	75 hrs	no	--
D	24 hrs	yes	Ru loss
E	76 hrs	no	--
F	8 hrs	yes	undetermined
G	<10 hrs	yes	undetermined

VI. CONCLUSIONS

RTO films were deposited onto niobium and Corning 7059 borosilicate glass substrates by reactive ion plating. The study demonstrates that a strong relationship exists between a MMO film's structure, chemistry, and electrochemical activity, and the processing techniques and parameters used to effect them.

Series C and E MMO films, comprised of 90 at.% titanium, 10 at.% ruthenium, and 80 at.% titanium, 20 at.% ruthenium, respectively, in the form of a dual phase mixture of RuO_2 and TiO_2 (rutile), were shown to exhibit the highest degree of electrochemical activity with respect to those films fabricated and tested for this study. Obtaining films with a dual phase mixture of RuO_2 and TiO_2 (rutile) with the correct proportions of ruthenium and titanium was shown to be a function of oxygen pressure, and ruthenium and titanium evaporation rates, the latter being qualitatively correlated to the respective electron beam gun currents. No dual phase mixture of RuO_2 and TiO_2 (rutile) was produced with average oxygen flow rates below 95 sccm. Solid solutions of ruthenium in TiO_2 (rutile) (series A) and TiO (cubic) (series B) formed with average oxygen flow rates of 61.1 sccm and 73.5 sccm, respectively. The formation of TiO_2 (anatase) with RuO_2 and TiO_2 (rutile) in series F and G films was linked to an intentional decrease in the ruthenium evaporation rate and thus to a lowering of the ruthenium, and RuO_2, content. It was suggested that an amount exceeding 5 at.% ruthenium may be required to stabilize the rutile form of TiO_2 in ion plated films comprised of RuO_2 and TiO_2.

As was alluded to above, films with a dual phase mixture of RuO_2 and TiO_2 (rutile) best displayed the ability to maintain a constant flow of current with little rise in applied potential over extended periods of time while subjected to anodic polarization conditions. Films comprised of solid solutions of TiO_2 (rutile) and ruthenium, or TiO (cubic) and ruthenium, displayed poor electrochemical activity under anodic polarization and were ineffective as impressed current anode materials. The presence of

TiO_2 (anatase), with the TiO_2 (rutile) and RuO_2 phases, diminished the MMO film's capability to withstand extreme anodic polarization conditions. Experimental data was presented suggesting the possibility that a TiO_2 (rutile)-to-TiO_2 (anatase) phase transformation is induced by anodic polarization in films containing both TiO_2 (anatase) and TiO_2 (rutile).

The mechanisms of film failure, analyzed with x-ray diffraction, electron diffraction, electron microprobe, inductively coupled argon plasma spectroscopy, and Auger electron spectroscopy, were shown to be related to ruthenium (and therefore RuO_2) depletion and substrate oxidation. ICAPS analysis of the electrolytes used in the anodic polarization of MMO films verified the presence of ruthenium in the electrolyte solution indicating that ruthenium may not oxidize to Ru^{8+} and form RuO_4 gas. The oxidation states of ruthenium ions in the analyzed electrolytes were not determined. Knowledge of these ruthenium oxidation states will help to assess the plausibility of potential RuO_4 formation. Subsequent work on the RuO_2 - TiO_2 system will include the use of an enhanced ICAPS program capable of determining ionic oxidation states.

It is unfortunate that the location of RuO_2, and its degree of homogeneity within the MMO films, was not determined. Scanning transmission electron microscopy will be used in future studies of this material system to identify the position of the RuO_2 and TiO_2 components within the MMO films to further characterize film microstructure and structure-property relationships. X-ray photoelectron spectroscopy (XPS) will also be performed in future analyses of the RuO_2 - TiO_2 system to determine the atomic bonding within the lattice. STEM and XPS information will be correlated to the observed electronic properties exhibited by RTO films to bring about a better understanding of the function of each of the film's components in electronic conduction and electrochemical activity. Additional SEM and TEM studies pertaining to the morphological, microstructural, and microchemical changes induced by anodic polarization will be performed in the future. Data from these studies will be used to further document specific changes in coating microstructure and chemistry brought on by anodic polarization.

Dissolution rates of polarized MMO films will be established in future work. In addition, corrosion properties of functioning MMO impressed current anodes will be studied to fully characterize their electrochemical behavior. The linear polarization technique will be performed to estimate a corrosion rate of the MMO films in various electrolytes; potentiodynamic polarization scans will be generated to gain knowledge of the film's corrosion behavior. SEM and TEM will be performed on these corrosion samples to document their morphology, microstructure, and crystal phases (via electron diffraction) prior to and following the polarization studies.

VII. REFERENCES

1. J. Morgan, Cathodic Protection, (Second Edition), Chapters 1, 5 (Houston, Texas: National Association of Corrosion Engineers, 1987).

2. M. G. Fontana and N. D. Greene, Corrosion Engineering, Chapter 6 (New York, New York: McGraw Hill, Inc., 1978).

3. H. B. Beer, United States Patent no. 3,632,498 (1972).

4. A. Kumar, E. G. Segan, and J. Bukowski, "Ceramic Coated Anode for Cathodic Protection," Materials Performance, (June, 1984) 24-28.

5. K. J. O'Leary and T. J. Navin, "Morphology of Dimensionally Stable Anodes," Chlorine Bicentennial Symposium, (The Electrochemical Society, Inc., 1974).

6. V. F. Hock, L. D. Stephenson, J. H. Givens, and J. M. Rigsbee, "Fabrication of Electrically Conductive Metal Oxide Coatings by Reactive Ion Plating," J. Vac. Sci. Technol., 3(6)(1985) 2661-2664.

7. E. G. Segan and A. Kumar, Army Technical Report CERL-TR-M-333 (1983).

8. Y. E. Roginskaya, V. I. Bystrov, and D. M. Shub, "X-ray Diffraction and Micro X-ray Spectrometric Investigations of the RuO_2-TiO_2-Cl System," Russian Journal of Inorganic Chemistry, 22(1)(1977) 110-113.

9. Y. E. Roginskaya, B. S. Galyamov, V. M. Lebedev, I. D. Belova, and Y. N. Venevtsev, "Phase Composition and Electrical Transport Properties of the RuO_2-TiO_2 System," Russian Journal of Inorganic Chemistry, 22(2)(1977) 273-276.

10. P. Triggs, H. Berger, C. A. Georg, and F. Levy, "Chemical Vapour Transport of Transition Metal Oxides (III) Crystal Growth of $Ti_{1-x}Ru_xO_2$ and Doped TiO_2," Mat. Res. Bull., 18(6)(1983) 677-681.

11. F. Hine, M. Yasuda, and T. Yoshida, "Studies on the Oxide-Coated Metal Anodes for Chlor-Alkali Cells," J. Electrochem Soc., 124(4)(1977) 500-505.

12. V. M. Lebedev, Y. E. Roginskaya, N. L. Klimasenko, V. I. Bystrov, and Y. N. Venevtsev, "Influence of the Method of Preparation on the Phase Composition of Specimens of the RuO_2-TiO_2 System," Russian Journal of Inorganic Chemistry, 21(9)(1976) 1380-1383.

13. W. A. Gerrard and B. C. H. Steele, "Microstructural Investigations on Mixed RuO_2-TiO_2 Coatings," J. Appl. Electrochem., 8(1978) 417-425.

14. L. Young, Anodic Oxide Films, Chapters 1-3 (New York, New York: Academic Press, 1961).

15. V. F. Hock, L. D. Stephenson, J. H. Givens, and J. M. Rigsbee, private communication with authors, U. S. Army Construction Engineering Research Laboratory, Champaign, Illinois, 1 September 1988.

16. T. Loucka, "The Reasons for the Loss of Activity of Titanium-Ruthenium Dioxide Anodes in Sulphuric Acid Media," J. Appl. Electrochem., 11(1981) 143-144.

17. L. M. Elina, V. M. Gitneva, V. I. Bystrov, and N. M. Shmigul, Elektrokhimiya, 10(1974) 68.

18. C. F. Schrieber and G. L. Mussinelli, "Characteristics and Performance of the Lida® Impressed Current System in Natural Waters and Saline Muds," Corrosion 86, (Houston, Texas: National Association of Corrosion Engineers, 1986).

19. D. M. Mattox, J. Appl. Phys., 34(1963) 2493.

20. D. M. Mattox, Proc. Conf. Ion Plating and Allied Techniques, (Edinburgh, UK: C. E. P. Consultants, 1979).

21. N. A. G. Ahmed, Ion Plating Technology, Developments and Applications (New York, New York: John Wiley & Sons Ltd., 1987).

22. D. L. Chambers and D. C. Carmichael, Research and Development Mag., 22(1971) 323.

23. D. G. Teer, Proc. Conf. Ion Plating and Allied Techniques, (Edinburgh, UK: C. E. P. Consultants, 1979) 13-31.

24. T. Spalvins, J. Vac. Sci. Technol., 17(1980) 315-321.

25. J. Machet, P. Saulnier, J. Ezquerra, and J. Guille, "Ion Energy Distribution in Ion Plating," Vacuum, 33(1983) 279.

26. B. Chapman, Glow Discharge Processes, (New York, New York: John Wiley & Sons, Inc., 1980).

27. J. A. Thornton, "Physical Vapor Deposition," G. E. McGuire, ed., Semiconductor Materials and Process Technologies, (Park Ridge, New Jersey: Noyes Publications, 1984).

28. P. Triggs, F. Levy, and F. E. Wagner, "Mossbauer Evidence for Ru(IV) and Ru(II) in TiO_2," Mat. Res. Bull., 19(1984) 197-200.

29. R. C. Weast, ed., CRC Handbook of Chemistry and Physics, (58th Edition) (West Palm Beach, Florida: CRC Press, Inc., 1978).

30. P. Kofstad, Nonstoichiometry, Diffusion, and Electrical Conductivity in Binary Metal Oxides, Chapter 8 (New York, New York: John Wiley & Sons, Inc., 1972).

31. L. I. Maissel and R. Glang, eds., Handbook of Thin Film Technology, Chapter 1 (New York, New York: McGraw-Hill, Inc., 1970).

32. L. D. Burke, J. F. Healy, and O. J. Murphy, "Corrosion of Oxide-Coated Titanium (DSA) Anodes in Organic Solvents (Especially Methanol)," J. Appl. Electrochem., 13(1983) 459-468.

33. J. A. Thornton, J. Vac. Sci. Technol., 4(6)(1986) 3059-3065.

34. T. Loucka, "The Reason for the Loss of Activity of Titanium Anodes Coated With a Layer of RuO_2 and TiO_2," J. Appl. Electrochem., 7(1977) 211-214.